

# Sampling-free parametric model reduction for structured systems

Christopher Beattie, Serkan Gugercin, and Zoran Tomljanović

November 25, 2021

## Abstract

We consider the reduction of parametric families of linear dynamical systems having an affine parameter dependence that differ from one another by a low-rank variation in the state matrix. Usual approaches for parametric model reduction typically involve exploring the parameter space to isolate representative models on which to focus model reduction methodology, which are then combined in various ways in order to interpolate the response from these representative models. The initial exploration of the parameter space can be a forbiddingly expensive task.

A different approach is proposed here that does not require any parameter sampling or exploration of the parameter space. Instead, we represent the system response in terms of four subsystems that are *nonparametric*. One may apply any one of a number of standard (nonparametric) model reduction strategies to reduce the subsystems independently, and then conjoin these reduced models with the underlying parameterized representation to obtain an overall parameterized response. Our approach has elements in common with the parameter mapping approach of Baur et al. [8], but offers greater flexibility and potentially greater control over accuracy. In particular, a data-driven variation of our approach is described that exercises this flexibility through the use of limited frequency-sampling of the underlying nonparametric models. The parametric structure of our system representation allows for *a priori* guarantees of system stability the resulting parametric reduced models, uniformly across all parameter values. Incorporation of system theoretic error bounds allow us to determine appropriate approximation orders for the nonparametric systems sufficient to yield uniformly high accuracy with respect to parameter variation.

We illustrate our approach on a class of structural damping optimization problems and on a benchmark model of thermal conduction in a semiconductor chip. The parametric structure of our reduced system representation lends itself very well to the development of optimization strategies making use of efficient cost function surrogates. We discuss this in some detail for damping parameter and location optimization for vibrating structures.

**Keywords:** parametric model reduction, sampling-free; damping optimization, structured systems

**Mathematics Subject Classification (2010):** 93C05; 49J15; 70Q05; 70H33

## 1 Introduction

Consider a linear time invariant dynamical system, parameterized with a  $k$ -dimensional parameter vector  $\mathbf{p} = [p_1, p_2, \dots, p_k]^T \in \Omega \subseteq \mathbb{R}^k$  and represented in state-space form as

$$\begin{aligned} E\dot{x}(t; \mathbf{p}) &= A(\mathbf{p})x(t; \mathbf{p}) + Bw(t), \\ y(t; \mathbf{p}) &= Cx(t; \mathbf{p}), \end{aligned} \tag{1}$$

where  $E, A(\mathbf{p}) \in \mathbb{R}^{n \times n}$ ,  $B \in \mathbb{R}^{n \times m}$  and  $C \in \mathbb{R}^{\ell \times n}$  are constant (time-invariant) matrices. In (1),  $x(t; \mathbf{p}) \in \mathbb{R}^n$ ,  $u(t) \in \mathbb{R}^m$  and  $y(t; \mathbf{p}) \in \mathbb{R}^\ell$  denote, the state vector, inputs, and outputs, respectively. We assume throughout that the matrix  $E$  is invertible.

## 1.1 Basic structure

The structural feature of the system that we will exploit extensively presumes that the system matrix  $A(\mathbf{p})$  has the parametric form

$$A(\mathbf{p}) = A_0 - U \operatorname{diag}(p_1, p_2, \dots, p_k) V^T = A_0 - \sum_{i=1}^k p_i u_i v_i^T, \quad (2)$$

where  $U = [u_1, u_2, \dots, u_k] \in \mathbb{R}^{n \times k}$  and  $V = [v_1, v_2, \dots, v_k] \in \mathbb{R}^{n \times k}$  are constant matrices with  $u_i, v_i \in \mathbb{R}^n$  for  $i = 1, \dots, k$ . Note that the parameterization in (2) is a special case of a general affine parametrization  $A(\mathbf{p}) = A_0 - \sum_i p_i A_i$  with the added rank constraint that the matrices  $A_i$  have rank-1. However, even for a general affine parametrization with  $A_i \in \mathbb{R}^{n \times n}$  individually having unrestricted rank but in aggregate having  $\operatorname{rank}(\sum_i p_i A_i) = k \ll n$ , the form of (2) may be assumed without loss of generality (allowing for the possibility that the parameters are replaced by functions of  $\{p_i\}_i$ ). The condition  $k \ll n$  is a practical constraint leading to the prospect of computational efficiency, but there is no theoretical restriction on the size of  $k$ .

Taking the Laplace transform of (1), the full-order transfer function of the parametrized system is obtained as

$$\mathcal{H}(s; \mathbf{p}) = C(sE - A(\mathbf{p}))^{-1}B = C(sE - (A_0 - U \operatorname{diag}(p_1, p_2, \dots, p_k) V^T))^{-1}B. \quad (3)$$

The goal of parametric model reduction, in this setting, is to find a reduced parametric system

$$\begin{aligned} E_r \dot{x}_r(t; \mathbf{p}) &= A_r(\mathbf{p}) x_r(t; \mathbf{p}) + B_r w(t), \\ y_r(t; \mathbf{p}) &= C_r x_r(t; \mathbf{p}), \end{aligned} \quad (4)$$

where  $E_r, A_r(\mathbf{p}) \in \mathbb{R}^{r \times r}$ ,  $B_r \in \mathbb{R}^{r \times m}$  and  $C_r \in \mathbb{R}^{\ell \times r}$  with  $r \ll n$  such that the reduced transfer function

$$\mathcal{H}_r(s; \mathbf{p}) = C_r(sE_r - A_r(\mathbf{p}))^{-1}B_r$$

approximates  $\mathcal{H}(s; \mathbf{p})$  accurately for the parameter range of interest.

Several approaches to parametric model order reduction (pMOR) exist. One of the most common approaches involves state-space projection using globally defined bases: Choose a set of parameter samples  $\mathbf{p}^1, \dots, \mathbf{p}^{n_s}$ . For every parameter sample  $\mathbf{p}^i$ , the full-order model  $\mathcal{H}(s; \mathbf{p}^i)$  becomes a non-parametric linear time-invariant system, for which a plethora of model reduction methods are available. Whatever choice is made, let  $Z_r^i$  and  $W_r^i$  denote the *local* model reduction bases for the parameter sample  $\mathbf{p}^i$ , for each  $i = 1, \dots, n_s$ . Then concatenate these local bases to form the *global* model reduction bases  $Z_r$  and  $W_r$ :  $Z_r = [Z_r^1, \dots, Z_r^{n_s}]$  and  $W_r = [W_r^1, \dots, W_r^{n_s}]$ . This concatenation step is usually followed by a rank-revealing *QR* or truncated SVD computation to compute and condense orthogonal bases. The parametric reduced model quantities in (4) are obtained via a Petrov-Galerkin projection, i.e.,

$$E_r = W_r^T E Z_r, \quad A_r(\mathbf{p}) = W_r^T A(\mathbf{p}) Z_r, \quad B_r = W_r^T B, \quad \text{and} \quad C_r = C Z_r. \quad (5)$$

Reviews of methods that consider such a reduction framework can be found, e.g. in [3, 4, 6, 9, 11, 13, 14, 16, 28, 58]. These approaches are widely studied especially for structured systems with particular applications; see, e.g., [6, 13–15, 58, 61, 63].

The global basis approach has been successfully applied in many circumstances requiring parametric model reduction and in some cases it may be the only viable approach. Nonetheless it comes with some drawbacks, the main issue being the need to sample the parameter domain adequately in order to construct representative local bases. Except for special cases [9, 33], how one chooses optimal parameter sampling points with respect to a joint global frequency-parameter error measure has not been known until recently. In [42], Hund et al. tackles this joint-optimization problem by deriving optimality conditions and then constructing model reduction bases that enforce those conditions. The most widely used approaches for global basis construction in pMOR are greedy or optimization-based sampling strategies; see [14] for a survey. However, especially in the case of high-dimensional parameter domains, this off-line stage could prove prohibitively expensive since it requires a large-number of full-order function evaluations. One may try to avoid these high-fidelity sampling techniques and pick parameter samples heuristically to make the off-line stage less costly. However, since the global bases directly depend on this initial sampling, which in turn influences

the final accuracy of the parametric reduced model, if this stage is not done properly the reduced model could not be expected to provide a good approximation over a wide parameter range.

In this paper, we focus on systems having the special structure described in (2). We develop a novel parametric model order reduction approach that is sampling free (that is, there is no need for parameter sampling) yet it still offers uniformly high fidelity across the full parameter range. Significantly, the reduced model retains the parametric structure of the original full model.

## 1.2 A motivating example: Damping optimization

Consider the vibrational system described by

$$\begin{aligned} M\ddot{q}(t) + D\dot{q}(t) + Kq(t) &= B_2w(t), \\ y(t) &= C_2q(t), \end{aligned} \quad (6)$$

where  $M$  and  $K$  are real, symmetric positive definite matrices of size  $n \times n$ , denoting the mass and stiffness matrices, respectively. The state variables are described by the coordinate vector  $q \in \mathbb{R}^n$  representing structure displacements. The time dependent vector  $w(t) \in \mathbb{R}^m$  is the primary excitation and typically represents an input disturbance.  $B_2 \in \mathbb{R}^{n \times m}$  is the *primary excitation matrix*, i.e., the input-to-state mapping. Similarly,  $y(t) \in \mathbb{R}^\ell$  is the performance output, representing a quantity of interest that is obtained from the state-vector  $q$  via a mapping by the state-output matrix  $C_2 \in \mathbb{R}^{\ell \times n}$ .

The damping matrix  $D \in \mathbb{R}^{n \times n}$  is modeled as

$$D = D_{int} + D_{ext},$$

where  $D_{ext}$  represents external damping and  $D_{int}$  represents internal damping. The internal damping  $D_{int}$  is usually taken to be a small multiple of the critical damping denoted by  $D_{crit}$  or a small multiple of proportional damping (see, e.g., [15, 19]):

$$D_{int} = \alpha_c D_{crit}, \quad \text{where} \quad D_{crit} = 2M^{1/2}\sqrt{M^{-1/2}KM^{-1/2}}M^{1/2}. \quad (7)$$

Other possibilities for modeling internal damping can be found, e.g., in [45].

We are mainly interested in the external damping of the type

$$D_{ext} = U_2 \text{diag}(p_1, p_2, \dots, p_k) U_2^T,$$

where the non-negative entries  $p_i$  for  $i = 1, \dots, k$  represent the friction coefficients of the dampers, usually called gains or viscosities, and the matrix  $U_2$  encodes the damper positions and geometry; for more details, see, e.g., [15, 18, 21, 48, 61, 62].

In damping optimization problems, the major goal is to determine *best/optimal* external damping matrix  $D_{ext}$  that will minimize the influence of the input  $w$  on the output  $y$ . One can consider different optimality measures. In the input-output dynamical systems settings, the optimization criteria are usually based on system norms such as  $\mathcal{H}_2$  or  $\mathcal{H}_\infty$  system norm (see, e.g., [15, 21]). Moreover, mixed performance measure that was introduced in [51]. This specific choice of optimization criteria strongly depends on the application at hand. pMOR methods we will develop in this paper will allow using different optimization criteria and therefore will enable different applications.

By defining the state-vector as  $x = [q^T \dot{q}^T]^T$  we obtain a first-order state-space representation of the vibrational system:

$$\begin{aligned} E\dot{x}(t) &= A(p)x(t) + Bw(t), \\ y(t) &= Cx(t), \end{aligned}$$

where

$$E = \begin{bmatrix} I & 0 \\ 0 & M \end{bmatrix}, \quad B = \begin{bmatrix} 0 \\ B_2 \end{bmatrix}, \quad C = [C_2 \quad 0], \quad (8)$$

$$\text{and} \quad A(p) = \underbrace{\begin{bmatrix} 0 & I \\ -K & -D_{int} \end{bmatrix}}_{A_0} - \underbrace{\begin{bmatrix} 0 \\ U_2 \end{bmatrix}}_U \text{diag}(p_1, p_2, \dots, p_k) \underbrace{\begin{bmatrix} 0 & U_2^T \end{bmatrix}}_{V^T = U^T}, \quad (9)$$

with  $\mathbf{p} = [p_1, p_2, \dots, p_k]^T$ . Note that the model for damping optimization in (8)-(9) has the parametric structure described in (2).

The optimization of damper locations can be formulated effectively as optimization over a finite (but potentially large) number of configurations for the matrix  $B_2$ ; this is a demanding combinatorial optimization problem and for each  $B_2$ -configuration, one must optimize over  $\mathbf{p}$ , the parameter vector. pMOR approaches seeking to make this task cheaper have been considered previously: For optimization based on the  $\mathcal{H}_2$  norm criterion, [15] used a global basis approach, as described above, where local bases were obtained via the dominant pole algorithm [59]. Using the same optimization criterion, [61] applied a global basis approach where local bases were obtained via the Iterative Rational Krylov Algorithm (IRKA) [36], an  $\mathcal{H}_2$ -optimal model reduction approach. Even though both approaches show great promise, success in each case depends on the initial parameter sampling used to construct the global basis, an issue that is faced in most pMOR cases. For the damping optimization problem, an efficient heuristic that can guide a parameter sampling strategy is not available, and the natural alternative, a preliminary offline greedy sampling stage, can be computationally very demanding and potentially negate the gains one would anticipate from model reduction.

In subsequent sections, we will propose two frameworks that will remove the need for parametric sampling in problems structured as in (2), including in particular the damping optimization problem discussed above. Thus, the new approach will allow efficient optimization of damping parameters encoded in the vector  $\mathbf{p}$ .

## 2 PMOR based on subsystem model reduction

In this section, we introduce our first sampling-free reduction method for the structured problem (3). We provide error bounds and also discuss the uniform stability of the reduced model.

### 2.1 Reformulation of the parametric transfer function

The crucial observation and the starting point behind our framework is that we can rewrite the structured transfer function (3) in a form that separates the  $s$  and  $\mathbf{p}$  dependency, by making use of the Sherman-Morrison-Woodbury formula [31]. We summarize this result in the following proposition.

**Proposition 1.** *Consider the structured transfer function*

$$\mathcal{H}(s; \mathbf{p}) = C (sE - (A_0 - U \operatorname{diag}(p_1, p_2, \dots, p_k) V^T))^{-1} B, \quad (10)$$

where  $p_i \in \mathbb{R}_+$ , for  $i = 1, 2, \dots, k$ . Then,

$$\mathcal{H}(s; \mathbf{p}) = \mathcal{H}_1(s) - \mathcal{H}_2(s) D(\mathbf{p}) [I + D(\mathbf{p}) \mathcal{H}_3(s) D(\mathbf{p})]^{-1} D(\mathbf{p}) \mathcal{H}_4(s), \quad (11)$$

where the diagonal matrix

$$D(\mathbf{p}) = \operatorname{diag}(\sqrt{p_1}, \sqrt{p_2}, \dots, \sqrt{p_k}) \quad (12)$$

encodes the parameters, and  $\mathcal{H}_1(s)$ ,  $\mathcal{H}_2(s)$ ,  $\mathcal{H}_3(s)$ , and  $\mathcal{H}_4(s)$  are non-parametric transfer functions given by

$$\begin{aligned} \mathcal{H}_1(s) &= C(sE - A_0)^{-1} B, & \mathcal{H}_2(s) &= C(sE - A_0)^{-1} U, \\ \mathcal{H}_3(s) &= V^T (sE - A_0)^{-1} U, \text{ and } & \mathcal{H}_4(s) &= V^T (sE - A_0)^{-1} B. \end{aligned} \quad (13)$$

*Proof.* Let  $T \in \mathbb{C}^{n \times n}$  be invertible. Also, let  $X \in \mathbb{C}^{n \times k}$  and  $Y \in \mathbb{C}^{n \times k}$  be such that  $I_k + Y^T T^{-1} X$  is invertible. Then, Sherman-Morrison-Woodbury formula states that

$$(T + XY^T)^{-1} = T^{-1} - T^{-1} X (I_k + Y^T T^{-1} X)^{-1} Y^T T^{-1}.$$

Recall that  $\mathcal{H}(s; \mathbf{p}) = C (sE - (A_0 - U \operatorname{diag}(p_1, p_2, \dots, p_k) V^T))^{-1} B$ . The result, then, follows from the Sherman-Morrison-Woodbury formula by defining  $T = sE - A_0$ ,  $X = UD(p)$ , and  $Y = VD(p)$ .  $\square$

**Remark 1.** Notice that if we define the extended parameterized transfer function

$$\tilde{\mathcal{F}}(s; \mathbf{p}) = \begin{bmatrix} \mathcal{H}_1(s) & \mathcal{H}_2(s)D(\mathbf{p}) \\ D(\mathbf{p})\mathcal{H}_4(s) & I + D(\mathbf{p})\mathcal{H}_3(s)D(\mathbf{p}) \end{bmatrix},$$

then (11) is the Schur complement of  $\tilde{\mathcal{F}}(s; \mathbf{p})$  with respect to the (2,2) block:

$$\mathcal{H}(s; \mathbf{p}) = \left[ \tilde{\mathcal{F}}(s; \mathbf{p}) / (I + D(\mathbf{p})\mathcal{H}_3(s)D(\mathbf{p})) \right].$$

**Remark 2.** Motivated by the damping optimization problem described in Section 1.2, Proposition 1 assumes that the parameter vector  $\mathbf{p}$  has positive entries, which lead to the form (11) where the diagonal matrix  $D(\mathbf{p})$  appear in a balanced symmetric way throughout the second term. However, the positive parameter range assumption is not necessary and the general case could be easily handled in a similar way. Define

$$\tilde{D}(\mathbf{p}) = \text{diag}(p_1, p_2, \dots, p_k).$$

Then,

$$\mathcal{H}(s; \mathbf{p}) = \mathcal{H}_1(s) - \mathcal{H}_2(s)\tilde{D}(\mathbf{p}) \left[ I + \mathcal{H}_3(s)\tilde{D}(\mathbf{p}) \right]^{-1} \mathcal{H}_4(s), \quad (14)$$

where  $\mathcal{H}_1(s)$ ,  $\mathcal{H}_2(s)$ ,  $\mathcal{H}_3(s)$ , and  $\mathcal{H}_4(s)$  are as defined in (13). In the rest of the paper, we will use the formulation in Proposition 1.2, but all the results to follow can be easily generalized using the form (14).

## 2.2 Subsystem model reduction

Proposition 1 displays a decomposition of the full-order transfer function  $\mathcal{H}(s; \mathbf{p})$  in terms of four *non-parametric* transfer functions with the parameter dependency entering as an interconnection coupling the four systems. Since  $\mathcal{H}_i(s)$ , for  $i = 1, 2, 3, 4$ , are non-parametric, they may be reduced without any need for sampling via well-established model reductions techniques such as balanced truncation (BT) [47, 49], Hankel norm approximation (HNA) [30], or iterative rational Krylov algorithm IRKA [36]; see [4, 6, 13] for further choices. Moreover, each system  $\mathcal{H}_i(s)$ , may be reduced independently of the others, potentially using different reduction orders and even different reduction methodologies.

Let the reduced model for  $\mathcal{H}_i(s)$  be denoted by  $\hat{\mathcal{H}}_i(s)$ , for  $i = 1, \dots, 4$ . The resulting parametric reduced model for  $\mathcal{H}(s; \mathbf{p})$  is given by

$$\mathcal{H}(s; \mathbf{p}) \approx \hat{\mathcal{H}}(s; \mathbf{p}) = \hat{\mathcal{H}}_1(s) - \hat{\mathcal{H}}_2(s)D(\mathbf{p})(I + D(\mathbf{p})\hat{\mathcal{H}}_3(s)D(\mathbf{p}))^{-1}D(\mathbf{p})\hat{\mathcal{H}}_4(s). \quad (15)$$

The online evaluation (or simulation) of  $\hat{\mathcal{H}}(s; \mathbf{p})$  for a given parameter value is trivial as it only involves reduced quantities and evaluation of the matrix  $D(\mathbf{p})$ . Therefore, we have constructed a parametric, easy-to-evaluate reduced model without any need for parameter sampling. Algorithm 1 below gives a sketch of this process.

---

### Algorithm 1 Parametric reduced order model based on reduction of subsystems

---

1: **Off-line Stage:** Calculate the four non-parametric reduced systems

$$\mathcal{H}_1(s) \rightarrow \hat{\mathcal{H}}_1(s), \quad \mathcal{H}_2(s) \rightarrow \hat{\mathcal{H}}_2(s), \quad \mathcal{H}_3(s) \rightarrow \hat{\mathcal{H}}_3(s), \quad \mathcal{H}_4(s) \rightarrow \hat{\mathcal{H}}_4(s),$$

(Reductions can be performed via a variety of nonparametric reduction techniques)

2: **On-line Stage:** For any given parameter  $\mathbf{p} = [p_1, p_2, \dots, p_k]^T$ , obtain the parametric model by

$$\mathcal{H}(s; \mathbf{p}) \approx \hat{\mathcal{H}}(s; \mathbf{p}) = \hat{\mathcal{H}}_1(s) - \hat{\mathcal{H}}_2(s)D(\mathbf{p})(I + D(\mathbf{p})\hat{\mathcal{H}}_3(s)D(\mathbf{p}))^{-1}D(\mathbf{p})\hat{\mathcal{H}}_4(s).$$


---

Some remarks are in order regarding Step 1 in Algorithm 1. The model  $\mathcal{H}_1(s)$  has the same input-output dimension as  $\mathcal{H}(s; \mathbf{p})$ . The model  $\mathcal{H}_2(s)$  has the same number of outputs ( $\ell$ ) as  $\mathcal{H}(s; \mathbf{p})$  and  $k$  inputs. Similarly, the model  $\mathcal{H}_4(s)$  has the same number of inputs ( $m$ ) as  $\mathcal{H}(s; \mathbf{p})$ , and also  $k$

outputs. Provided that the input/output dimension is modest, reducing  $\mathcal{H}_1(s)$ ,  $\mathcal{H}_2(s)$ , and  $\mathcal{H}_4(s)$  will not be expected to be strongly influenced by the size of  $k$  since in most cases the smaller of the input/output dimensions determines the difficulty in reducing a dynamical systems. On the other hand, the model  $\mathcal{H}_3(s)$  will have  $k$ -inputs and  $k$ -outputs. Therefore, if  $k$  is significantly larger than  $\ell$  or  $m$ , this is likely to be the most difficult model to reduce with high fidelity. Therefore, although the framework and theoretical analysis we develop here apply to a system with transfer function

$$\mathcal{H}(s; \mathbf{p}) = C(sE - (A_0 - pA_1))^{-1}B$$

even when  $A_1$  has full rank, computational difficulties might arise since  $\mathcal{H}_3(s)$  will then be an  $n$ -dimension dynamical system with  $n$ -inputs and  $n$ -outputs. Such models will not generally be amenable to model reduction in most scenarios.

Next we provide an error bound for the parametric model reduction due to Algorithm 1.

**Theorem 1.** *Let the full order transfer function  $\mathcal{H}(s; \mathbf{p})$ , and the corresponding subsystems  $\mathcal{H}_i(s)$ , for  $i = 1, \dots, 4$  be given as in (11) and (13). Assume that the nonparametric reduced models  $\hat{\mathcal{H}}_i(s)$  are reduced so that*

$$\|\mathcal{H}_i - \hat{\mathcal{H}}_i\| \leq \epsilon_i, \quad \text{for } i = 1, \dots, 4, \quad (16)$$

*and that the corresponding parametric reduced model  $\hat{\mathcal{H}}(s; \mathbf{p})$  is constructed as in (15). Then,*

$$\|\mathcal{H}(\cdot; \mathbf{p}) - \hat{\mathcal{H}}(\cdot; \mathbf{p})\| \leq \epsilon_1 + f_1(\mathbf{p}, \hat{\mathcal{H}}_3, \hat{\mathcal{H}}_4)\epsilon_2 + f_1(\mathbf{p}, \hat{\mathcal{H}}_3, \hat{\mathcal{H}}_4)f_2(\mathbf{p}, \mathcal{H}_2, \mathcal{H}_3)\epsilon_3 + f_2(\mathbf{p}, \mathcal{H}_2, \mathcal{H}_3)\epsilon_4 \quad (17)$$

where

$$f_1(\mathbf{p}, \mathcal{G}_1, \mathcal{G}_2) = \|D(\mathbf{p})(I + D(\mathbf{p})\mathcal{G}_1(\cdot)D(\mathbf{p}))^{-1}D(\mathbf{p})\mathcal{G}_2(\cdot)\|, \quad \text{and} \quad (18)$$

$$f_2(\mathbf{p}, \mathcal{G}_1, \mathcal{G}_2) = \|\mathcal{G}_1(\cdot)D(\mathbf{p})(I + D(\mathbf{p})\mathcal{G}_2(\cdot)D(\mathbf{p}))^{-1}D(\mathbf{p})\|. \quad (19)$$

*Proof.* First, by using the formulae (11) and (15), we obtain

$$\mathcal{H}(s; \mathbf{p}) - \hat{\mathcal{H}}(s; \mathbf{p}) = \mathcal{H}_1(s) - \hat{\mathcal{H}}_1(s) + \hat{\mathcal{H}}_2(s)\hat{\mathcal{E}}_1 - \mathcal{H}_2(s)\mathcal{E}_1, \quad (20)$$

where  $\mathcal{E}_1 = D(\mathbf{p})(I + D(\mathbf{p})\mathcal{H}_3(s)D(\mathbf{p}))^{-1}D(\mathbf{p})\mathcal{H}_4(s)$  and  $\hat{\mathcal{E}}_1 = D(\mathbf{p})(I + D(\mathbf{p})\hat{\mathcal{H}}_3(s)D(\mathbf{p}))^{-1}D(\mathbf{p})\hat{\mathcal{H}}_4(s)$ . The last two terms can be manipulated as

$$\begin{aligned} \hat{\mathcal{H}}_2(s)\hat{\mathcal{E}}_1 - \mathcal{H}_2(s)\mathcal{E}_1 &= [\hat{\mathcal{H}}_2(s) - \mathcal{H}_2(s)]\hat{\mathcal{E}}_1 + \mathcal{H}_2(s)(\hat{\mathcal{E}}_1 - \mathcal{E}_1) \\ &= [\hat{\mathcal{H}}_2(s) - \mathcal{H}_2(s)]\hat{\mathcal{E}}_1 + \mathcal{H}_2(s)[\hat{\mathcal{E}}_2\hat{\mathcal{H}}_4(s) - \mathcal{E}_2\mathcal{H}_4(s)], \end{aligned}$$

where  $\mathcal{E}_2 = D(\mathbf{p})(I + D(\mathbf{p})\mathcal{H}_3(s)D(\mathbf{p}))^{-1}D(\mathbf{p})$  and  $\hat{\mathcal{E}}_2 = D(\mathbf{p})(I + D(\mathbf{p})\hat{\mathcal{H}}_3(s)D(\mathbf{p}))^{-1}D(\mathbf{p})$ . This last expression can be rewritten as

$$\hat{\mathcal{H}}_2(s)\hat{\mathcal{E}}_1 - \mathcal{H}_2(s)\mathcal{E}_1 = [\hat{\mathcal{H}}_2(s) - \mathcal{H}_2(s)]\hat{\mathcal{E}}_1 + \mathcal{H}_2(s)[(\hat{\mathcal{E}}_2 - \mathcal{E}_2)\hat{\mathcal{H}}_4(s) + \mathcal{E}_2(\hat{\mathcal{H}}_4(s) - \mathcal{H}_4(s))]. \quad (21)$$

Next consider the term  $\mathcal{E}_2 - \hat{\mathcal{E}}_2$ , which can be expressed as

$$\hat{\mathcal{E}}_2 - \mathcal{E}_2 = D(\mathbf{p})(I + D(\mathbf{p})\hat{\mathcal{H}}_3(s)D(\mathbf{p}))^{-1}D(\mathbf{p})[\mathcal{H}_3(s) - \hat{\mathcal{H}}_3(s)]D(\mathbf{p})(I + D(\mathbf{p})\mathcal{H}_3(s)D(\mathbf{p}))^{-1}D(\mathbf{p}). \quad (22)$$

Substituting (22) into (21), which is then substituted into (20), yields

$$\begin{aligned} \mathcal{H}(\cdot; \mathbf{p}) - \hat{\mathcal{H}}(\cdot; \mathbf{p}) &= [\mathcal{H}_1(s) - \hat{\mathcal{H}}_1(s)] + [\mathcal{H}_2(s) - \hat{\mathcal{H}}_2(s)]D(\mathbf{p})(I + D(\mathbf{p})\hat{\mathcal{H}}_3(s)D(\mathbf{p}))^{-1}D(\mathbf{p})\hat{\mathcal{H}}_4(s) \\ &\quad + \mathcal{H}_2(s)D(\mathbf{p})(I + D(\mathbf{p})\mathcal{H}_3(s)D(\mathbf{p}))^{-1}D(\mathbf{p})[\hat{\mathcal{H}}_4(s) - \mathcal{H}_4(s)] + \\ &\quad + \mathcal{H}_2(s)D(\mathbf{p})(I + D(\mathbf{p})\mathcal{H}_3(s)D(\mathbf{p}))^{-1}D(\mathbf{p})[\mathcal{H}_3(s) - \hat{\mathcal{H}}_3(s)] \\ &\quad \cdot D(\mathbf{p})(I + D(\mathbf{p})\hat{\mathcal{H}}_3(s)D(\mathbf{p}))^{-1}D(\mathbf{p})\hat{\mathcal{H}}_4(s). \end{aligned}$$

The upper bound follows by taking norms on both sides.  $\square$



## 2.3 Uniform stability of the parametric reduced model

In many applications, the full model  $\mathcal{H}(s, \mathbf{p})$  in (10) is asymptotically stable for every  $\mathbf{p} \in \Omega$ , so that eigenvalues of the matrix pencil  $\lambda E - A(\mathbf{p})$  (poles of the transfer function  $\mathcal{H}(s, \mathbf{p})$ ) have negative real parts for every  $\mathbf{p} \in \Omega$ . The damping optimization problem we considered in Section 1.2 is one such example where the underlying physical phenomenon is asymptotically stable for every parameter in the parameter domain of interest. Therefore, it is reasonable to expect the same of the parametric reduced model. We will call this *uniform asymptotic stability* of the reduced model. Unfortunately, except for some special cases (e.g.,  $E = E^T$  is positive definite,  $A(\mathbf{p}) = A^T(\mathbf{p})$  is negative definite, and one chooses  $W_r = Z_r$  in (5)), this property is difficult to enforce. We refer the reader to [14, §5.4] for a brief discussion on this issue. We show here that our proposed framework will guarantee uniform stability for a significantly broader class of problems.

Recall the damping optimization model with the space-state quantities defined in (8)-(9). Due to the internal damping term,  $D_{int}$ , eigenvalues of the matrix pencil  $sE - A_0$  have negative real parts; and thus all the subsystems, i.e.,  $\mathcal{H}_1(s)$ ,  $\mathcal{H}_2(s)$ ,  $\mathcal{H}_3(s)$ , and  $\mathcal{H}_4(s)$ , are asymptotically stable. Then, in reducing these nonparametric subsystems, we can enforce stability preservation by employing, for example, BT [47, 49], HNA [30], or IRKA with stability enforcement [12, 35, 36]. Therefore, starting point of our uniform stability result is that all the subsystems are asymptotically stable, as is in the damping optimization problem.

To further motivate the setting of our uniform stability result, next we inspect the term  $\mathcal{H}_3(s)$  more closely for the damping optimization problem. It directly follows from (8) and (9) that the transfer function  $\mathcal{H}_3(s)$  is given by  $\mathcal{H}_3(s) = sU_2^T(s^2M + sD + K)^{-1}U_2$ , which corresponds to a positive real (passive) dynamical system. In other words,  $\text{Re}(\mathcal{H}_3(s)) \geq 0$  for all  $s$  with  $\text{Re}(s) \geq 0$ . Therefore,  $I + D(\mathbf{p})\mathcal{H}_3(s)D(\mathbf{p})$  is strictly positive real, i.e.,  $\text{Re}(\mathcal{H}_3(s)) > 0$  for  $\text{Re}(s) \geq 0$ . Using positive real balanced truncation [24, 52] or interpolatory port-Hamiltonian model reduction [27, 37, 57], one can reduce  $\mathcal{H}_3(s)$  in a way to retain positive realness. Motivated by these structures and observations appearing in the damping optimization problem, we now state the uniform stability result.

**Theorem 2.** *Consider the full parametric model with its transfer function  $\mathcal{H}(s)$  written in terms of the subsystems as in (10) where the subsystems  $\mathcal{H}_1(s)$ ,  $\mathcal{H}_2(s)$ , and  $\mathcal{H}_4(s)$  are asymptotically stable. Further assume that  $\mathcal{H}_3(s)$  is positive real. Construct the reduced subsystems  $\hat{\mathcal{H}}_1(s)$ ,  $\hat{\mathcal{H}}_2(s)$ , and  $\hat{\mathcal{H}}_4(s)$  such that they retain asymptotic stability, and  $\hat{\mathcal{H}}_3(s)$  such that it retains positive-realness. Then, the reduced parametric model  $\hat{\mathcal{H}}(s)$  in (15) is uniformly asymptotically stable for every  $\mathbf{p} \in \Omega$ .*

*Proof.* It follows from the structure of the reduced transfer function  $\hat{\mathcal{H}}(s, \mathbf{p})$  in (15) that its poles are composed of the poles of  $\hat{\mathcal{H}}_1(s)$ ,  $\hat{\mathcal{H}}_2(s)$ , and  $\hat{\mathcal{H}}_4(s)$ , and the zeroes of  $I + D(\mathbf{p})\hat{\mathcal{H}}_3(s)D(\mathbf{p})$ . Note that the poles of  $\hat{\mathcal{H}}_1(s)$ ,  $\hat{\mathcal{H}}_2(s)$ , and  $\hat{\mathcal{H}}_4(s)$  are independent of  $\mathbf{p}$  and all have negative real parts since these subsystems are asymptotically stable as they have been obtained via a model reduction algorithm to enforce this property. Therefore, these poles cannot contribute to potential instability and what is left to verify is that the zeroes of  $I + D(\mathbf{p})\hat{\mathcal{H}}_3(s)D(\mathbf{p})$  have negative real parts for every  $\mathbf{p} \in \Omega$ . Recall that  $\hat{\mathcal{H}}_3(s)$  was constructed with a positive-realness preserving model reduction technique. Therefore,  $I + D(\mathbf{p})\hat{\mathcal{H}}_3(s)D(\mathbf{p})$  is *strictly* positive real for every  $\mathbf{p} \in \Omega$  and cannot lose rank in the right-half plane, i.e., it does not have a zero in the right-half plane. Indeed,  $I + D(\mathbf{p})\hat{\mathcal{H}}_3(s)D(\mathbf{p})$  is a minimum-phase system, meaning all of its poles and zeros have negative real parts. Then, put together with the poles of  $\hat{\mathcal{H}}_1(s)$ ,  $\hat{\mathcal{H}}_2(s)$ , and  $\hat{\mathcal{H}}_4(s)$ , the reduced transfer function  $\hat{\mathcal{H}}(s, \mathbf{p})$  is uniformly asymptotically stable. Note that there could be further pole-zero cancellations in the construction of  $\hat{\mathcal{H}}(s, \mathbf{p})$ . However, this will not change the conclusion since all the poles (before any potential pole-zero cancellation) already have negative real parts.  $\square$

**Remark 3.** *One approach to guarantee uniform asymptotic stability in the general case was proposed by Baur and Benner [10] where  $\mathcal{H}(s, \mathbf{p})$  is sampled at some parameter values  $\mathbf{p}^i$  for  $i = 1, 2, \dots, n_s$  and reduced using stability preserving reduction such as BT. Then, the final parametric reduced system is obtained by connecting these local reduced models via interpolation in the  $\mathbf{p}$ -domain. Since the interpolation in the  $\mathbf{p}$ -domain does not affect the poles, the resulting reduced parametric system is uniformly asymptotically stable. However, this comes at the cost of poles being fixed, i.e., the poles do not vary with the parameters since the  $\mathbf{p}$ -dependency is completely in the  $B$ - or  $C$ -matrix. The situation is different in our formulation where the poles still vary with  $\mathbf{p}$ ,*

as desired, yet remain uniformly asymptotically stable. Moreover, the main motivation behind our approach here is to avoid the need for parameter sampling.

**Remark 4.** Theorem 2 implies that in the case of the damping optimization problem (and others with similar structure), we can construct a sampling-free parametric reduced model that is uniformly asymptotically stable with an error bound.

### 2.3.1 Uniform asymptotic stability in the general case

Theorem 2 provided uniform asymptotic stability for the case when  $\mathcal{H}_3(s)$  is a positive real transfer function. What can we state about stability in the general case without this structure?

We will continue to assume that all the subsystems are asymptotically stable and we apply an appropriate model reduction technique so that all the reduced subsystems are asymptotically stable as well. Following the proof of Theorem 2, we only need to check the zeroes of  $I + D(\mathbf{p})\hat{\mathcal{H}}_3(s)D(\mathbf{p})$  and argue that these zeroes have negative real parts.

To see the arguments more easily, let us consider the case that the parameter  $\mathbf{p}$  is a scalar,  $D(\mathbf{p}) = \sqrt{\mathbf{p}}$ ,  $U$  and  $V$  are column vectors, and thus  $\mathcal{H}_3(s)$  is a single-input/single-output dynamical system. In this case, if  $z_0$  is zero of  $1 + D(\mathbf{p})\hat{\mathcal{H}}_3(s)D(\mathbf{p})$ , then  $\hat{\mathcal{H}}_3(z_0) = -1/\mathbf{p}$ . Let  $\mathbf{p}_{\max}$  denote  $\mathbf{p}_{\max} = \sup_{\mathbf{p} \in \Omega} |\mathbf{p}|$ . A sufficient condition for such a  $z_0$  not to exist is that  $\|\hat{\mathcal{H}}_3\|_{\mathcal{H}_\infty} < \frac{1}{\mathbf{p}_{\max}}$ . Assuming that this condition holds for  $\mathcal{H}_3(s)$ , which will guarantee that the full model is uniformly asymptotically stable, one can apply bounded real balancing [52, 54] in constructing  $\hat{\mathcal{H}}_3(s)$  so that it has the same  $\mathcal{H}_\infty$ -norm bound. The general case, i.e., when  $\mathbf{p}$  is a vector, follows similarly and we list this result as a corollary.

**Corollary 1.** Consider the full parametric model with its transfer function  $\mathcal{H}(s)$  written in terms of the subsystems as in (10) where all the subsystems  $\mathcal{H}_i(s)$  for  $i = 1, \dots, 4$  are asymptotically stable. Let  $\mathbf{p}_{\max}$  denote  $\mathbf{p}_{\max} = \sup_{\mathbf{p} \in \Omega} \|\mathbf{p}\|_\infty$  and assume that  $\mathcal{H}_3(s)$  satisfies  $\|\mathcal{H}_3\|_{\mathcal{H}_\infty} < \frac{1}{\mathbf{p}_{\max}}$ . Construct the reduced subsystems  $\hat{\mathcal{H}}_1(s)$ ,  $\hat{\mathcal{H}}_2(s)$ , and  $\hat{\mathcal{H}}_4(s)$  such that they retain asymptotic stability, and  $\hat{\mathcal{H}}_3(s)$  such that it retains the property  $\|\hat{\mathcal{H}}_3\|_{\mathcal{H}_\infty} < \frac{1}{\mathbf{p}_{\max}}$ . Then, the reduced parametric model  $\hat{\mathcal{H}}(s)$  in (15) is uniformly asymptotically stable for every  $\mathbf{p} \in \Omega$ .

## 2.4 The parameter mapping approach of Baur et al. [8]

The parameterization given in (2) appears as a (relatively) low rank change from the base dynamic matrix,  $A_0$ , and it is this structural feature that we have exploited. Another strategy that exploits this parametric structure has been proposed in [8]. There, one augments and modifies the system by introducing a set of  $k$  additional synthetic inputs,  $\omega(t)$ , and outputs,  $\eta(t)$ , in such a way that the internal system parameterization is mapped to a feedthrough term. The original system response is recovered by constraining the synthetic inputs so as to null the synthetic outputs. The modified system can be reduced independently of the parameterization and the final parameterized reduced model is recovered by imposing an analogous constraint on the synthetic inputs; they are chosen to null the (reduced) synthetic outputs. To illustrate, define

$$\begin{aligned} E\dot{x}(t) &= A_0x + [B \quad UD(\mathbf{p})] \begin{bmatrix} w(t) \\ \omega(t) \end{bmatrix}, \\ \begin{bmatrix} \hat{y}(t) \\ \eta(t) \end{bmatrix} &= \begin{bmatrix} C \\ D(\mathbf{p})V^T \end{bmatrix} x(t) + \begin{bmatrix} 0 \\ I \end{bmatrix} \begin{bmatrix} w(t) \\ \omega(t) \end{bmatrix}. \end{aligned} \quad (23)$$

Evidently, this system has  $m + k$  inputs,  $\ell + k$  outputs, and the parameterization now acts on a  $k$  dimensional subpace that is common to both input and output spaces. Notice in particular that the parameterization no longer acts directly on the state vector. What relation does the response of (23) have with that of the original system (2)? If  $\omega(t)$  is chosen so that  $\eta(t) = 0$  (for example, if  $\omega(t)$  is assigned by state feedback as  $\omega(t) = -D(\mathbf{p})V^T x(t)$ ), then the remaining output  $\hat{y}(t)$  matches the output of the parameterized system described in (2):  $\hat{y}(t) = y(t; \mathbf{p})$ . Indeed, with this added constraint imposed on the synthetic inputs, the transfer function for the resulting system is identical to what has been defined by (10).

The dynamical system described in (23) may be reduced using any strategy appropriate for linear time-invariant MIMO (multiple input/multiple output) systems. Since the parameterization has been mapped to the synthetic input/output spaces and is now external to system dynamics,



model reduction strategies can be pursued without the need of any parameter sampling. The approach described in [8] proposes a projective reduced model derived, say, as in (4)-(5) using projection bases defined by  $Z_r$  and  $W_r$ :

$$\begin{aligned} E_r \dot{x}_r(t) &= A_{0r} x_r + [B_r \quad W_r^T U D(\mathbf{p})] \begin{bmatrix} w(t) \\ \hat{\omega}(t) \end{bmatrix}, \\ \begin{bmatrix} \hat{y}_r(t) \\ \eta_r(t) \end{bmatrix} &= \begin{bmatrix} C_r \\ D(\mathbf{p}) V^T Z_r \end{bmatrix} x_r(t) + \begin{bmatrix} 0 \\ I \end{bmatrix} \begin{bmatrix} w(t) \\ \hat{\omega}(t) \end{bmatrix}. \end{aligned} \quad (24)$$

Following [8], we set up a state feedback constraint to null the reduced synthetic outputs, similar to what has gone before. If  $\hat{\omega}(t)$  is assigned via reduced state feedback as  $\hat{\omega}(t) = -D(\mathbf{p}) V^T Z_r x_r(t)$ , then  $\eta_r(t) = 0$ , and the reduced output  $\hat{y}_r(t)$  will define the output of a reduced parametric system (2):  $y_r(t; \mathbf{p}) = \hat{y}_r(t)$ . The state-space representation of the resulting reduced model is given by

$$W_r^T E Z_r \dot{x}_r(t) = W_r^T A_0 Z_r x_r - W_r^T U D^2(\mathbf{p}) Z_r + W_r^T B w(t) \quad (25)$$

$$\hat{y}_r(t) = C Z_r x_r(t) \quad (26)$$

To make a clearer connection to our proposed framework, we re-write the transfer function of this reduced dynamical system equivalent as in (15) as

$$\hat{\mathcal{H}}(s; \mathbf{p}) = \hat{\mathcal{H}}_1(s) - \hat{\mathcal{H}}_2(s) D(\mathbf{p}) (I + D(\mathbf{p}) \hat{\mathcal{H}}_3(s) D(\mathbf{p}))^{-1} D(\mathbf{p}) \hat{\mathcal{H}}_4(s).$$

In this case each system,  $\mathcal{H}_i(s)$ , is reduced with the projection bases,  $Z_r$  and  $W_r$ , for  $i = 1, 2, 3, 4$ ; that is, the *same projection bases* are used for all four systems.

Although the approach we take here is evidently closely aligned with the approach of [8], an important distinction is that we are able here to reduce the individual subsystems,  $\mathcal{H}_i(s)$ , independently of one another. This allows us to better control the fidelity of the final model, and as we described in Section 2.3, we are able to guarantee asymptotic stability of  $\hat{\mathcal{H}}(s; \mathbf{p})$  uniformly in  $\mathbf{p}$ , so long as each reduced model  $\hat{\mathcal{H}}_i(s)$ ,  $i = 1, 2, 3, 4$  is asymptotically stable and the single reduced  $\hat{\mathcal{H}}_3(s)$  is also positive real. Naturally, these assertions may also be made with the approach of [8] or its recent formulation for second-order systems [55], but it can be substantially more difficult to guarantee these properties using a single choice of projecting bases,  $Z_r$  and  $W_r$ . We are able to exploit the flexibility of reducing the four subsystems independently of one another and do not suffer under these constraints.

## 2.5 Numerical Examples

We will illustrate the performance of Algorithm 1 on two numerical examples. In both examples, subsystem reduction was performed by BT. Since the subsystems have the same  $E$ -term and  $A$ -term, only one (Schur) decomposition in the offline stage, Step 1, of Algorithm 1 is needed. Therefore Step 1 is significantly cheaper than applying BT to four different systems.

**Example 1.** We consider the parametric version of the Penzl model [43, 56]. The full model transfer function  $\mathcal{H}(s, \mathbf{p}) = C(sE - A(\mathbf{p}))^{-1}B$  is defined by the quantities  $E = I$ ;

$$A = \text{diag}(A(p_1), A(p_2), A(p_3), -1, -2, \dots, -M),$$

$$\text{where } A(p_i) = \begin{bmatrix} -1 & p_i \\ -p_i & -1 \end{bmatrix}, \quad \text{for } i = 1, \dots, 3;$$

$$C = [c_1 \ c_2 \ \dots \ c_M] \in \mathbb{R}^{1 \times (M+6)} \quad \text{where } c_i = \begin{cases} 10, & i = 1, \dots, 6 \\ 1, & i = 7, \dots, M; \end{cases} \quad \text{and } B = C^T.$$

The parameters  $p_1, p_2, p_3$  represent magnitude of the imaginary parts of the two eigenvalues of the diagonal block  $A(p_i)$ , for  $i = 1, 2, 3$ , respectively and they control the location of the peaks in the frequency response.

This linear time invariant system can be equivalently represented in the structured form (2) with

$$A(\mathbf{p}) = A_0 - U \text{diag}(p_1, p_1, p_2, p_2, p_3, p_3) V^T,$$

where  $A_0 = \text{diag}(I_6, -1, -2, \dots, -M)$ ;  $v_i = e_i$  for  $i = 1, \dots, 6$  where  $e_i$  is the  $i$ th canonical vector; and similarly

$$u_i = \begin{cases} -e_{i+1}, & i = 1, 3, 5, \\ e_{i-1}, & i = 2, 4, 6. \end{cases}$$

We chose  $M = 100$ , which implies  $n = 106$ . This modest dimension is not necessary as BT can be applied in much higher dimensions. It is chosen just to illustrate the theoretical considerations. Based on the Hankel singular values of  $\mathcal{H}_i(s)$ , for  $i = 1, \dots, 4$ , in Step 1 of Algorithm 1, we obtain reduced subsystems  $\hat{\mathcal{H}}_i(s)$  with dimensions  $r_1 = 10$ ,  $r_2 = 1$ ,  $r_3 = 6$ , and  $r_4 = 1$ , respectively. This is an advantage of the proposed framework: reduction of subsystems and their reduced orders are independent of each other.

We compare  $\mathcal{H}(s, \mathbf{p})$  and  $\hat{\mathcal{H}}(s, \mathbf{p})$  by inspecting them on the imaginary axis; i.e.,  $|\mathcal{H}(i\omega, \mathbf{p})|$  vs  $|\hat{\mathcal{H}}(i\omega, \mathbf{p})|$  where  $i = \sqrt{-1}$  and  $\omega \in \mathbb{R}$ . The top plot in Figure 1 shows the quality of the approximation for the fixed parameters  $(p_1, p_2, p_3) = (10, 100, 5000)$  and illustrates that the reduced model approximates the full model very accurately. The relative error in the approximation, i.e.,  $\frac{|\mathcal{H}(i\omega, \mathbf{p}) - \hat{\mathcal{H}}(i\omega, \mathbf{p})|}{\max_{\omega} |\mathcal{H}(i\omega, \mathbf{p})|}$  is presented in the bottom plot of Figure 1. Note that this reduced model is obtained without any parameter sampling.

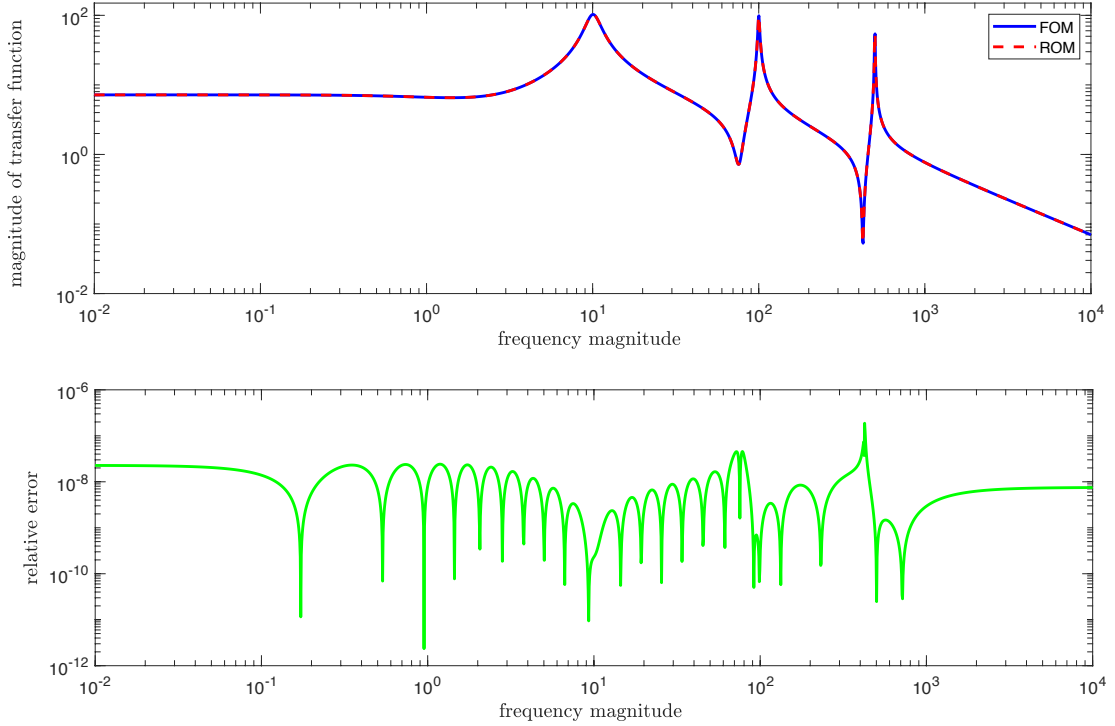


Figure 1: Transfer function plot and relative error for  $(p_1, p_2, p_3) = (10, 100, 5000)$

It is not enough that  $\hat{\mathcal{H}}(s, \mathbf{p})$  is accurate for one parameter set. In order to illustrate the quality of approximation and its ability to approximate the system for different parameters, we consider different configurations of parameters  $p_1, p_2, p_3$ . As mentioned earlier, the parameters control the imaginary part of the complex poles and different parameter selections will move these peaks in the frequency domain. In Figure 2 we present the surface plot that illustrates  $|\mathcal{H}(i\omega, \mathbf{p})|$ , as in Figure 1 but for different parameters  $p_1, p_2, p_3$ . In order to obtain a three-dimensional surface plot, we choose

$$(p_1, p_2, p_3) = (\mathbf{p}, 10\mathbf{p}, 50\mathbf{p}), \quad \text{with } \mathbf{p} \in [1, 100]. \quad (27)$$

On the top plot in Figure 2 we show  $|\mathcal{H}(i\omega, \mathbf{p})|$ , illustrating how the peaks are moving with the parameter  $\mathbf{p}$ . The lower subplot shows magnitude of relative errors for all considered parameters

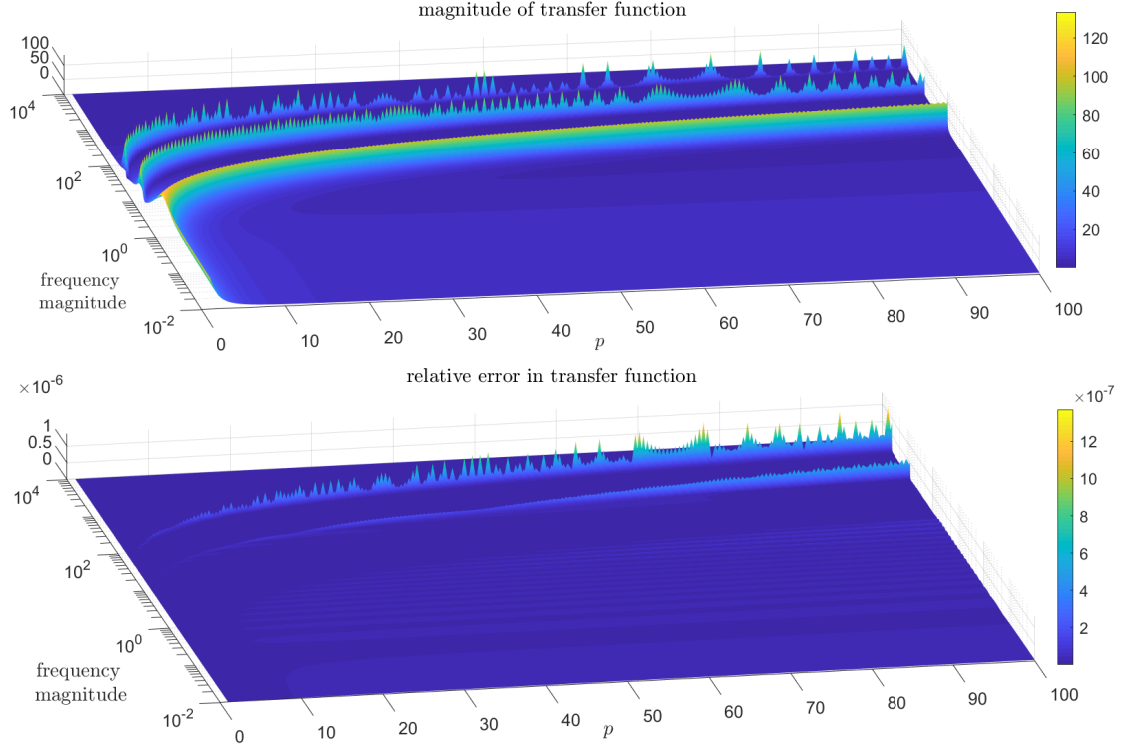


Figure 2: Magnitude of transfer function and relative error for parameters given by (27)

and illustrates that the reduced model is accurate across the parameter domain (27), with the largest relative error being less than  $10^{-6}$ . This accuracy is obtained by performing four non-parametric model reductions without any parameter sampling. We finally note that the reduced model  $\hat{\mathcal{H}}(s, \mathbf{p})$  is obtained to be asymptotically stable for every parameter sample.

**Example 2.** In We consider a model from the Oberwolfach Benchmark Collection representing thermal conduction in a semiconductor chip [53]. The full model is described by

$$\begin{aligned} E\dot{x} &= (A - p_t A_t - p_b A_b - p_s A_s)x + Bu, \\ y &= Cx, \end{aligned}$$

where  $E \in \mathbb{R}^{4257 \times 4257}$  represents the heat capacity and  $A \in \mathbb{R}^{4257 \times 4257}$  the heat conductivity. The matrices  $A_t, A_b, A_s \in \mathbb{R}^{4257 \times 4257}$  are diagonal matrices resulting from the discretization of the convection boundary conditions with ranks 111, 99, and 31, respectively. The matrix  $B \in \mathbb{R}^{1 \times 4257}$  is the load vector and  $C \in \mathbb{R}^{7 \times 4257}$  is the output matrix, while the parameters  $p_t, p_b, p_s$  represent the film coefficients. For further details for the model, we refer the reader to [29, 53].

We fix  $p_t = 1000$  and vary both  $p_b$  and  $p_s$  between 1 and  $10^9$ ; so here we have  $\mathbf{p} = [p_b \ p_s]$ . This model can be written in our structured parametric form as in (2) with  $A_0 = A - p_t A_t$ , for the fixed  $p_t = 1000$ , and  $U$  and  $V$  are matrices with  $\text{rank}(U) = \text{rank}(V) = \text{rank}(A_b) + \text{rank}(A_s) = 130$ .

Based on the Hankel singular values, we reduce  $\mathcal{H}_i(s)$  to  $\hat{\mathcal{H}}_i(s)$  via BT using reduced orders  $r_1 = 46, r_2 = 66, r_3 = 200$ , and  $r_4 = 16$ . The reduced order  $r_3$  is bigger than the others as expected since it corresponds to approximating a dynamical system with 130 inputs and 130 outputs. In Figure 3, we illustrate the quality of the approximation obtained by Algorithm 1 over the full parameter domain using the  $\mathcal{H}_2$ -measure, i.e.,  $\|H(\cdot, \mathbf{p})\|_{\mathcal{H}_2} = \sqrt{\frac{1}{2\pi} \int_{-\infty}^{\infty} \|\mathcal{H}(j\omega, \mathbf{p})\|_F^2 d\omega}$  (we will revisit system norms in Section 4). In Figure 3, the  $x$  and  $y$  axes represent, respectively, the parameters  $p_s$  and  $p_t$ , and the  $z$ -axis shows the relative error  $\frac{\|\mathcal{H}(\cdot; \mathbf{p}) - \hat{\mathcal{H}}(\cdot; \mathbf{p})\|_{\mathcal{H}_2}}{\|\mathcal{H}(\cdot; \mathbf{p})\|_{\mathcal{H}_2}}$  for the reduced system  $\hat{\mathcal{H}}(s, \mathbf{p})$  calculated by Algorithm 1. It is clear from the figure that  $\hat{\mathcal{H}}(s, \mathbf{p})$  is accurate

across the full parameter domain, with relative error smaller than  $2.4 \times 10^{-6}$  for all parameters in  $(p_s, p_b) \in [1, 10^9]^2$ . This high-fidelity approximation is obtained at the cost of four non-parametric subsystem model reduction without parameter sampling. As in the previous example,  $\hat{\mathcal{H}}(s, \mathbf{p})$  is asymptotically stable for every parameter sample.

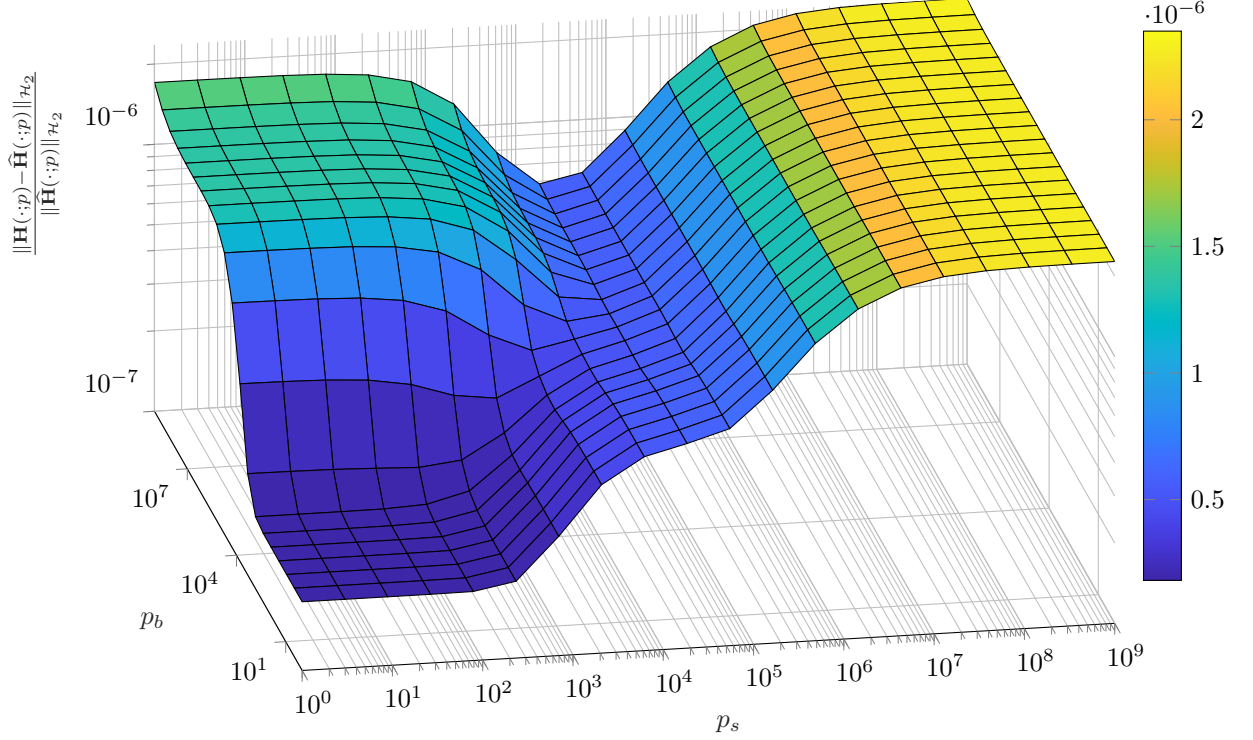


Figure 3: Relative error for different parameters for thermal model

### 3 Data-driven PMOR with subsystem frequency sampling

In Section 2, we proposed a sampling-free parametric model reduction approach that involved the preliminary reduction of four non-parametric models. In this section we will present a second approach that depends on the same four systems yet uses a data-driven framework based on transfer function (frequency-domain) samples to construct parametric reduced models in the offline stage. We will first briefly review data-driven modeling frameworks and then present the main approach.

#### 3.1 Data-driven modeling from transfer function samples

Let  $\mathcal{H}(s)$  denote the transfer function of a (nonparametric) linear dynamical system.  $\mathcal{H}(s)$  need not be a rational function of  $s$  and can contain, for example, internal delays or other non-rational dependence in  $s$ . Assume that we have access to samples of this transfer function, i.e., we have  $\mathcal{H}(\xi_1), \mathcal{H}(\xi_2), \dots, \mathcal{H}(\xi_N)$  where  $\xi_i \in \mathbb{C}$  for  $i = 1, 2, \dots, N$  are the sampling points. When obtained experimentally, these sampling points are chosen on the imaginary axis. If an analytical evaluation of  $\mathcal{H}(s)$  is possible, they can be chosen arbitrarily as long as they do not coincide with the poles of  $\mathcal{H}(s)$ . In our numerical experiments, we will work with samples on the imaginary axis but the theoretical discussion applies to the general case.

Data-driven modeling in this case amounts to the following question: Given the samples  $\{\mathcal{H}(\xi_i)\}_{i=1}^N$  (without access to internal dynamics of  $\mathcal{H}(s)$ , i.e., without access to a state-space transformation), construct a rational approximation  $\hat{\mathcal{H}}(s)$  of degree- $r$  that fits the data in an appropriate sense. There are various ways to fit this frequency domain data. One can enforce  $\hat{\mathcal{H}}(s)$  to interpolate the data at every sampling point using the Loewner framework [5, 46], or construct  $\hat{\mathcal{H}}(s)$  to fit the data in a least-squares (LS) sense [20, 25, 39], or force  $\hat{\mathcal{H}}(s)$  to interpolate some of

the data and while minimizing the LS fit in the rest [50]. In this paper, we will fit data solely in a LS sense.

Therefore, given the samples  $\{\mathcal{H}(\xi_i)\}_{i=1}^N$ , our goal is to construct a degree- $r$  rational function  $\hat{\mathcal{H}}(s)$ , i.e., a reduced transfer function, that minimizes the LS error  $\sum_{i=1}^N \|\mathcal{H}(\xi_i) - \hat{\mathcal{H}}(\xi_i)\|_F^2$ . Note

that due to the nonlinear dependence on the poles of  $\hat{\mathcal{H}}(s)$ , this is a nonlinear LS problem. There are various approaches for solving this problem, see, e.g., [20, 25, 32, 39, 41, 50, 60]. Our approach employs the Vector Fitting (VF) framework of [39] even though one can easily adapt any of the other LS methods. We view VF as a tool to be employed (as we did with BT and IRKA in subsystem reduction approach of Section 2) and therefore we do not explain it in detail. VF uses the barycentric-form of  $\hat{\mathcal{H}}(s)$ , as opposed to a state-space formulation, and converts the nonlinear LS problem into a sequence of weighted linear LS problems each of which could be solved easily by well-established numerical linear algebra tools in every step. The variables in each step are the coefficients of the barycentric form. Once the iteration is terminated, a state-space form is recovered. For details, we refer the reader to, for example, [23, 26, 38, 39], [34, Chap 7] and the references therein.

We make a brief remark regarding computational cost: VF performs  $m \cdot \ell$  QR factorizations of size  $N \times (2r)$  in every step [26]. When  $m$  and  $\ell$  are modest, say  $m, \ell < 10$ , this is not a big computational effort. The cost will increase as  $m$  and  $\ell$  grow; however there are various ways to speed up the process such as performing the  $m \cdot \ell$  QR factorizations in parallel [23, 38] as they are independent of each other. We have not needed any such sophisticated tools and a basic implementation proved efficient for us. Assume that the underlying system is a rational function itself; i.e.,  $\mathcal{H}(s) = C(sE - A)^{-1}B$ . Then, obtaining the samples  $\{\mathcal{H}(\xi_i)\}_{i=1}^N$  require solving  $N$  linear systems of size  $n \times n$  with multiple right-hand size; a much larger cost compared to VF itself. Therefore, the main cost of VF is indeed the sampling step itself.

### 3.2 pMOR from offline samples

Now, we discuss how we integrate the subsystem structure revealed in Proposition 1 and VF for the parametric problems with the structured transfer function  $\mathcal{H}(s, \mathbf{p})$ . As we briefly discussed above, the main cost in VF comes from computing the transfer function samples at selected frequencies. Therefore, we want to avoid re-sampling  $\mathcal{H}(s, \mathbf{p})$  from scratch for every given  $\mathbf{p}$ .

Recall (11), which we repeat below

$$\mathcal{H}(s; \mathbf{p}) = \mathcal{H}_1(s) - \mathcal{H}_2(s)D(\mathbf{p})[I + D(\mathbf{p})\mathcal{H}_3(s)D(\mathbf{p})]^{-1}D(\mathbf{p})\mathcal{H}_4(s).$$

Given the predetermined points  $\xi_1, \dots, \xi_N$  in the complex plane, compute the samples

$$\mathcal{H}_1(\xi_i), \mathcal{H}_2(\xi_i), \mathcal{H}_3(\xi_i), \mathcal{H}_4(\xi_i) \quad \text{for } i = 1, \dots, N.$$

It is important to note that these values do not depend on parameter  $\mathbf{p}$ , which means that we can perform this computation once in the off-line stage. Furthermore, all four subsystem transfer functions share the same resolvent  $(sE - A_0)^{-1}$ ; therefore in evaluating  $\mathcal{H}_j(\xi_i)$  for  $j = 1, \dots, n$ , one takes advantage of this fact, significantly reducing the numerical cost of this step.

Then, for a parameter  $\mathbf{p}$ , using (11) we can efficiently calculate the values  $\mathcal{H}(\xi_i; \mathbf{p})$  as

$$\mathcal{H}(\xi_i; \mathbf{p}) = \mathcal{H}_1(\xi_i) - \mathcal{H}_2(\xi_i)D(\mathbf{p})(I + D(\mathbf{p})\mathcal{H}_3(\xi_i)D(\mathbf{p}))^{-1}D(\mathbf{p})\mathcal{H}_4(\xi_i), \quad (28)$$

for  $i = 1, \dots, N$ . This step comes essentially at no cost. Therefore, we can re-sample  $\mathcal{H}(\xi_i; \mathbf{p})$  for any  $\mathbf{p}$  with almost no effort. Then, a data-driven approach, such as VF can be employed to construct a reduced model at a desired parameter value. This is summarized in Algorithm 2.

For determining the quality of the approximation resulting from Algorithm 2, we will use discrete LS error. That is, we will use the error measure calculated by

$$e(\mathcal{H}(\cdot; \mathbf{p}), \hat{\mathcal{H}}(\cdot; \mathbf{p})) = \sum_{i=1}^N \left\| \mathcal{H}(\xi_i; \mathbf{p}) - \hat{\mathcal{H}}(\xi_i; \mathbf{p}) \right\|_F^2. \quad (29)$$

Similar to Algorithm 1, sampling-based Algorithm 2 is well suited for computationally efficient parameter optimization and studying important system properties. In Algorithm 2, Step 1 is

---

**Algorithm 2** Parametric reduced order model based on VF

---

1: Off-line Stage: For the predetermined points in the complex plane  $\xi_1, \dots, \xi_N$  calculate

$$\mathcal{H}_1(\xi_i), \mathcal{H}_2(\xi_i), \mathcal{H}_3(\xi_i), \mathcal{H}_4(\xi_i) \quad \text{for } i = 1, \dots, N,$$

using (13).

2: On-line Stage:

For any given parameter  $\mathbf{p}$  calculate  $\mathcal{H}(\xi_i; \mathbf{p})$  for  $i = 1, \dots, N$  using formula (28).

3: Based on  $\mathcal{H}(\xi_1; \mathbf{p}), \dots, \mathcal{H}(\xi_N; \mathbf{p})$  obtain reduced system  $\hat{\mathcal{H}}(s; \mathbf{p})$  using VF.

---

executed only once in the off-line stage. Then, each time the parameter  $\mathbf{p}$  is varied, (in the on-line stage), steps 2-3 can be executed efficiently. In the next section, we will present how one can use Algorithms 1 and 2, and the error estimates given by (17) and (29), to ensure robust and accurate parameter optimization.

## 4 Parameter optimization for systems with low-rank parameterization

In this section we will present algorithms for parameter optimization problems that inherit the dynamical structure in (2). We will incorporate the proposed sampling-free parametric model reduction techniques of Sections 2 and 3 into these optimization problems for efficient surrogate optimization.

Parameter optimization plays a vital role in many applications. In the case of damping optimization setting, this is computationally demanding problem even for moderate dimensions. The main reason lies in the fact that we need to optimize damping parameters (viscosities) together with damping positions that is a demanding combinatorial optimization problem. Optimization of damping parameters for the case of criteria based on system norms was studied, e.g., in [15, 21, 51, 61]. In this section we will present algorithms that allow parameter optimization in structured systems and in the section with numerical experiments we will apply these algorithms for efficient optimization of damping parameters. For usage of model reduction in optimization in more general settings, we refer the reader to, e.g., [1, 2, 7, 17, 22, 40, 44, 64] and the references therein.

### 4.1 The choice of cost function in damping optimization

Consider the following ODE-constrained optimization problem:

$$\begin{aligned} \mathbf{p}^* &= \arg \min_{\mathbf{p} \in \Omega} \|y(\cdot, \mathbf{p})\| \\ \text{subject to } \quad & E\dot{x}(t; \mathbf{p}) = A(\mathbf{p})x(t; \mathbf{p}) + Bu(t), \\ & y(t; \mathbf{p}) = Cx(t; \mathbf{p}). \end{aligned} \tag{30}$$

There are many viable choices for the norm selection  $\|y(\cdot, \mathbf{p})\|$  and the algorithms we describe below will apply to these various scenarios. However, with the damping optimization problem of Section 1.2 in mind we will choose a specific norm discussed below.

Recall that in the damping optimization setting, the input  $w$  represents an input disturbance and the goal is to minimize the influence of  $w$  on the output  $y$ . Therefore, one might choose to minimize  $\|y(\cdot, \mathbf{p})\|_{L_\infty} := \sup_{t \geq 0} \|y(t, \mathbf{p})\|_\infty$  or  $\|y(\cdot, \mathbf{p})\|_{L_2} := \sqrt{\int_0^\infty \|y(t, \mathbf{p})\|_2^2 dt}$ . These norms can be equivalently represented using the transfer function  $\mathcal{H}(s, \mathbf{p})$ . The corresponding frequency-domain norms are the  $\mathcal{H}_2$  and  $\mathcal{H}_\infty$  norms:

$$\|\mathcal{H}(\cdot, \mathbf{p})\|_{\mathcal{H}_2} := \sqrt{\frac{1}{2\pi} \int_{-\infty}^{\infty} \|\mathcal{H}(i\omega, \mathbf{p})\|_F^2 d\omega} \quad \text{and} \quad \|\mathcal{H}(\cdot, \mathbf{p})\|_{\mathcal{H}_\infty} := \sup_{\omega \in \mathbb{R}} \|\mathcal{H}(i\omega, \mathbf{p})\|_2, \tag{31}$$

where  $i^2 = -1$  and  $\|\cdot\|_F$  denotes the Frobenius norm. For a stable linear (parametric) dynamical systems with an input  $w(t)$  having  $\|w\|_{L_2} \leq \infty$  and the corresponding output  $y(t; \mathbf{p})$ , it holds

$$\|y(\cdot, \mathbf{p})\|_{L_\infty} \leq \|\mathcal{H}(\cdot, \mathbf{p})\|_{\mathcal{H}_2} \|w\|_{L_2} \quad \text{and} \quad \|y(\cdot, \mathbf{p})\|_{L_2} \leq \|\mathcal{H}(\cdot, \mathbf{p})\|_{\mathcal{H}_\infty} \|w\|_{L_2}.$$



Therefore the optimization problem (30), with the choice of the  $L_\infty$  norm, can be equivalently rewritten as

$$\mathbf{p}^* = \arg \min_{\mathbf{p} \in \Omega} \|\mathcal{H}(\cdot, \mathbf{p})\|_{\mathcal{H}_2} \quad \text{where} \quad \mathcal{H}(s, \mathbf{p}) = C(sE - (A_0 - U D^2(\mathbf{p}) V^T))^{-1} B. \quad (32)$$

In the discussion below, we will present the analysis and algorithms for the parameter optimization problem (32).

## 4.2 Surrogate optimization with reduced parametric models

The major cost in (32) is the computation of the  $\mathcal{H}_2$  norm. For  $\mathcal{H}(s; \mathbf{p}) = C(sE - A(\mathbf{p}))^{-1}B$ , the  $\mathcal{H}_2$  norm is computed by solving a Lyapunov equation:

$$\|\mathcal{H}(\cdot, \mathbf{p})\|_{\mathcal{H}_2} = \sqrt{\text{trace}(CPC^T)} \quad \text{where } P \text{ solves } A(\mathbf{p})PE^T + EPA(\mathbf{p})^T + BB^T = 0.$$

Solving a large-scale Lyapunov equation is computationally demanding and in this optimization setting one has to repeat this task for many different  $\mathbf{p}$  values. We will use the parametric reduced models from Algorithms 1 and 2 to relieve this computational burden. Therefore, as opposed to (32), we will solve the surrogate optimization problem

$$\hat{\mathbf{p}}^* = \arg \min_{\mathbf{p} \in \Omega} \|\hat{\mathcal{H}}(\cdot, \mathbf{p})\|_{\mathcal{H}_2}, \quad (33)$$

where the reduced parametric transfer function  $\hat{\mathcal{H}}(\cdot, \mathbf{p})$  will be constructed as in either Algorithm 1 or Algorithm 2, without need for parameter sampling.

Assume  $\mathbf{p}^*$  is the minimizer of (32) and note that

$$\|\mathcal{H}(\cdot, \mathbf{p}^*)\|_{\mathcal{H}_2} \leq \|\mathcal{H}(\cdot, \mathbf{p}^*) - \hat{\mathcal{H}}(\cdot, \mathbf{p}^*)\|_{\mathcal{H}_2} + \|\hat{\mathcal{H}}(\cdot, \mathbf{p}^*)\|_{\mathcal{H}_2}. \quad (34)$$

The surrogate optimization problem (33) will minimize the second term in (34). Therefore, we need to verify that the first term in (34) is small enough. In other words, we need the reduced model  $\hat{\mathcal{H}}(s, \mathbf{p})$  to be an accurate approximation at the minimizer  $\hat{\mathbf{p}}^*$ .

### 4.2.1 Surrogate optimization with reduced model via Algorithm 1

To guarantee that  $\hat{\mathcal{H}}(s, \mathbf{p})$  is accurate enough at the optimizer  $\hat{\mathbf{p}}^*$ , we need to evaluate the term  $\|\mathcal{H}(\cdot, \hat{\mathbf{p}}^*) - \hat{\mathcal{H}}(\cdot, \hat{\mathbf{p}}^*)\|_{\mathcal{H}_2}$ . Therefore, an efficient evaluation (estimation) of this term during optimization is crucial for a numerically effective implementation.

When Algorithm 1 is employed to construct the reduced model  $\hat{\mathcal{H}}(s, \mathbf{p})$ , Theorem 1, more specifically (17), shows how  $\|\mathcal{H}(\cdot, \hat{\mathbf{p}}^*) - \hat{\mathcal{H}}(\cdot, \hat{\mathbf{p}}^*)\|_{\mathcal{H}_2}$  can be bounded using the subsystem errors  $\epsilon_i = \|\mathcal{H}_i(\cdot) - \hat{\mathcal{H}}_i(\cdot)\|$ , for  $i = 1, 2, 3, 4$ . Unfortunately, two of the terms in (17) depend on the full order quantities  $\mathcal{H}_1(s)$  and  $\mathcal{H}_2(s)$ . Therefore, in our surrogate optimization routine, we will use an approximation to this upper bound. Assuming  $\hat{\mathcal{H}}_2(s)$  and  $\hat{\mathcal{H}}_3(s)$  are accurate approximations to  $\mathcal{H}_2(s)$  and  $\mathcal{H}_3(s)$ , i.e.,  $\mathcal{H}_2 \approx \hat{\mathcal{H}}_2$ , and  $\mathcal{H}_3 \approx \hat{\mathcal{H}}_3$  (note that we can control this accuracy in the model reduction stage), using Theorem 1, we will approximate the upper bound as

$$\begin{aligned} \|\mathcal{H}(\cdot; \mathbf{p}) - \hat{\mathcal{H}}(\cdot; \mathbf{p})\| &\lesssim \epsilon_1 + \epsilon_2 f_1(\mathbf{p}, \hat{\mathcal{H}}_3, \hat{\mathcal{H}}_4) \\ &\quad + \epsilon_3 f_1(\mathbf{p}, \hat{\mathcal{H}}_3, \hat{\mathcal{H}}_4) f_2(\mathbf{p}, \hat{\mathcal{H}}_2, \hat{\mathcal{H}}_3) + \epsilon_4 f_2(\mathbf{p}, \hat{\mathcal{H}}_2, \hat{\mathcal{H}}_3), \end{aligned} \quad (35)$$

where functions  $f_1$  and  $f_2$  are given by (18) and (19), respectively, and  $\epsilon_i = \|\mathcal{H}_i(\cdot) - \hat{\mathcal{H}}_i(\cdot)\|$  for  $i = 1, \dots, 4$ . To simplify the notation, we will denote the upper bound estimate, i.e., the right hand-side of (35), with  $f(\mathbf{p})$ .

Now, using  $f(\mathbf{p})$ , we can efficiently estimate the accuracy of the reduced model at a given parameter value  $\mathbf{p}$ . In Algorithm 3, we give an outline of a surrogate optimization method using this estimate. Starting with initial reduced subsystems in Step 1 (constructed for a given accuracy), Algorithm 3 solves the surrogate optimization problem in Step 2. Then, Step 3 checks whether the reduced model is accurate enough at the current optimizer using the estimate  $f(\mathbf{p})$  for the upper

---

**Algorithm 3** Surrogate parameter optimization using reduced models via Algorithm 1

---

**Require:** System matrices  $A(\mathbf{p}), E, B, C$  defining (1);

initial point  $\mathbf{p}^0$  for optimization routine

tolerance  $0 < \tau \ll 1$  for error bound

tolerance  $0 < \nu \ll 1$  for optimization routine

starting reduced dimensions  $r_1, r_2, r_3, r_4$  and the corresponding subsystems  $\hat{\mathcal{H}}_1, \hat{\mathcal{H}}_2, \hat{\mathcal{H}}_3$ , and  $\hat{\mathcal{H}}_4$ .

**Ensure:** approximation of optimal parameters

- 1: Choose the reduced orders  $r_1, r_2, r_3, r_4$  (and thus the reduced subsystems  $\hat{\mathcal{H}}_1(s), \hat{\mathcal{H}}_2(s), \hat{\mathcal{H}}_3(s)$ , and  $\hat{\mathcal{H}}_4(s)$  via Algorithm 1) so that  $f(\mathbf{p}^0) < \tau$ .
- 2: Solve the surrogate optimization problem

$$\hat{\mathbf{p}}^* = \arg \min_{\mathbf{p}} \left\| \hat{\mathcal{H}}(\cdot, \mathbf{p}) \right\|_{\mathcal{H}_2}$$

with the initial guess  $\mathbf{p}^0$  and tolerance  $\nu$ .

- 3: **while** minimizer  $\mathbf{p}^*$  such that  $f(\mathbf{p}^*) > \tau$  **do**

- 4:  $\mathbf{p}^0 = \hat{\mathbf{p}}^*$

- 5: Increase the reduced orders  $r_1, r_2, r_3, r_4$  (and thus the reduced subsystems via Algorithm 1) so that  $f(\hat{\mathbf{p}}^*) < \tau$ .

- 6: Determine the new minimizer by solving the surrogate optimization problem

$$\hat{\mathbf{p}}^* = \arg \min_{\mathbf{p}} \left\| \hat{\mathcal{H}}(\cdot, \mathbf{p}) \right\|_{\mathcal{H}_2}$$

using the updated  $\hat{\mathcal{H}}$ , the initial guess  $\mathbf{p}^0$ , and tolerance  $\nu$ .

- 7: **end while**

---

bound. If it is, the algorithm terminates. Otherwise, Step 5 adaptively increases the reduced dimension and Step 6 resolves the surrogate optimization for the updated reduced model. This procedure is repeated until desired tolerance is met.

There are various algorithmic details that will help speed up the computations. We will not dive into those details; instead highlight some points. For example, assume that subsystem model reduction in Algorithm 1 is performed using BT. Then, to increase the reduced dimensions in Step 5, one does not need to apply model reduction from scratch. In the case of BT, one will only need to add more vectors to the BT-based model reduction bases from already computed quantities. If IRKA is employed in Algorithm 1, then the current reduced-model poles, appended with some others, will be an effective initialization strategy for IRKA, yielding faster convergence.

#### 4.2.2 Surrogate optimization with reduced model via Algorithm 2

We now focus on solving the optimization problem (32) using reduced models from the data-driven Algorithm 2. One major difference from Algorithm 1 is that in this case there are no reduced subsystems. Instead, for every given  $\mathbf{p}$ , we have a numerically efficient way to find an accurate approximation  $\hat{\mathcal{H}}(s, \mathbf{p})$  to  $\mathcal{H}(s, \mathbf{p})$ . Therefore, the subsystem-based error estimate in (35) does not apply here. However, we have the sample-based (discretized) version  $e(\mathbf{p})$  defined in (29). For example, if VF is employed in Algorithm 2, the error  $e(\mathbf{p})$  will be automatically calculated during the construction of  $\hat{\mathcal{H}}(s, \mathbf{p})$  and thus no additional effort is needed to compute  $e(\mathbf{p})$ . Therefore, following similar arguments to those found in Section 4.2.1, in solving the surrogate optimization problem (33), we need to ensure that the reduced model  $\hat{\mathcal{H}}(s, \mathbf{p})$  is an accurate approximation to  $\mathcal{H}(s, \mathbf{p})$  at the optimizer  $\mathbf{p} = \hat{\mathbf{p}}^*$  where accuracy is now measured using  $e(p)$ .

The resulting approach is briefly discussed in Algorithm 4. The fundamental structure is almost identical to that of Algorithm 3. We test whether  $e(\hat{\mathbf{p}}^*)$  is below a prespecified tolerance. If not, we increase the order of the reduced model in Algorithm 2 until we reach the desired accuracy.

As is the case with Algorithm 3, there are various numerical aspects that one could exploit to make the online computations faster. For example, one main factor determining the convergence speed of VF is an initial selection of poles. In the damping optimization problem, the poles from the critical damping case, are perfect candidates. Also, if one has to increase the order in Step 5 of Algorithm 4, the already-converged poles from the previous optimization step (appended with a

---

**Algorithm 4** Surrogate parameter optimization using reduced models via Algorithm 2
 

---

**Require:** System matrices  $A(\mathbf{p}), E, B, C$  defining (1);

initial point  $\mathbf{p}^0$  for optimization routine

tolerance  $0 < \tau \ll 1$  for error bound

tolerance  $0 < \nu \ll 1$  for optimization routine

Samples  $\{\mathcal{H}_i(\xi_i)\}_{i=1}^N$  at predetermined points in the complex plane  $\xi_1, \dots, \xi_N$ .

**Ensure:** approximation of optimal parameters

1: Choose the reduced order in Algorithm 2 so that  $e(\mathbf{p}^0) < \tau$ .

2: Solve the surrogate optimization problem

$$\hat{\mathbf{p}}^* = \arg \min_{\mathbf{p}} \left\| \hat{\mathcal{H}}(\cdot, \mathbf{p}) \right\|_{\mathcal{H}_2}$$

with the initial guess  $\mathbf{p}^0$  and tolerance  $\nu$  with  $\hat{\mathcal{H}}_{\mathbf{p}}$  computed via Algorithm 2 using samples  $\{\mathcal{H}_i(\xi_i)\}_{i=1}^N$ .

3: **while** minimizer  $\mathbf{p}^*$  such that  $e(\mathbf{p}^*) > \tau$  **do**

4:    $\mathbf{p}^0 = \hat{\mathbf{p}}^*$

5:   Increase the reduced order used in Algorithm 2 so that  $e(\mathbf{p}^*) < \tau$ .

6:   Determine the new minimizer by solving the surrogate optimization problem

$$\hat{\mathbf{p}}^* = \arg \min_{\mathbf{p}} \left\| \hat{\mathcal{H}}(\cdot, \mathbf{p}) \right\|_{\mathcal{H}_2}$$

using the updated  $\hat{\mathcal{H}}$ , the initial guess  $\mathbf{p}^0$ , and tolerance  $\nu$ .

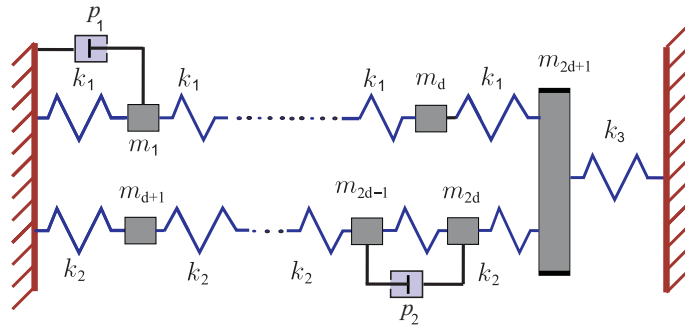
7: **end while**

---

small number of additional ones) is certainly expected to speed up convergence. We will elaborate on these points in the numerical example below.

### 4.3 Numerical Example

We revisit the damping optimization problem described in Section 1.2 and focus on optimizing the viscosities for different sets of damping positions. We consider an  $n$ -mass oscillator with  $n = 2d + 1$  masses and  $2d + 3$  springs as shown in Figure 4.3. This oscillator has two rows of  $d$  masses connected with springs. The leading masses in each row on the left edge are connected to a fixed boundary while on the opposite (right) edge the masses ( $m_d$  and  $m_{2d}$ ) are connected to a single mass  $m_{2d+1}$ , which, in turn, is connected to a fixed boundary. See [15, 61] for further details.



The state-space model is given by (6) where the stiffness matrix is given by

$$K = \begin{bmatrix} K_{11} & & -\kappa_1 \\ & K_{22} & -\kappa_2 \\ -\kappa_1^T & -\kappa_2^T & k_1 + k_2 + k_3 \end{bmatrix}, \quad K_{ii} = k_i \begin{bmatrix} 2 & -1 & & \\ -1 & 2 & -1 & \\ & \ddots & \ddots & \ddots \\ & & -1 & 2 & -1 \\ & & & -1 & 2 \end{bmatrix},$$

with  $\kappa_i = [0 \quad \dots \quad 0 \quad k_i]$  for  $i = 1$  and  $i = 2$ , and the mass matrix is  $M = \text{diag}(m_1, m_2, \dots, m_n)$ .

We pick  $n = 1801$  masses ( $d = 900$ ) with the values

$$m_i = \begin{cases} 1000 - \frac{i}{2}, & i = 1, \dots, 450, \\ i + 325, & i = 451, \dots, 900, \\ 1300 - \frac{i}{4}, & i = 901, \dots, n. \end{cases}$$

The stiffness values are chosen as  $k_1 = 500, k_2 = 200$ , and  $k_3 = 300$ . The parameter  $\alpha_c$  that determines the influence of the internal damping defined by (7) is set to 0.02. The primary excitation corresponds to five masses closest to ground, i.e.,  $B_2 \in \mathbb{R}^{n \times 5}$  with

$$\begin{aligned} B_2(1 : 2, 1 : 2) &= \text{diag}(20, 10), \\ B_2(901 : 902, 3 : 4) &= \text{diag}(20, 10), \\ B_2(1801, 5) &= 30; \end{aligned}$$

and all other entries being zero. We are interested in the two displacements, yielding the output

$$y(t; p) = [q_{400}(t; p) \quad q_{1300}(t; p)]^T.$$

In this example we consider optimization over four dampers with gains  $p_1, p_2, p_3$  and  $p_4$  with their positions encoded in

$$U_2 = [e_{j_1} - e_{j_1+10}, \quad e_{j_2}, \quad e_{j_3}, \quad e_{j_3} - e_{j_3+100}],$$

where  $e_i$  is the  $i$ th canonical vector and the indices  $j_1, j_2, j_3$  determine the damping positions. In order to illustrate the performance of our surrogate optimization framework for different damping configurations, the following indices are considered:  $j_1 \in \{100, 300, 500, 700\}$ ,  $j_2 \in \{150, 350, 550, 750\}$ , and  $j_3 \in \{1400, 1700\}$ . This results in 32 different damping configurations for which we optimize  $\mathcal{H}_2$  system norm, i.e., we solve (32) and the surrogate problem (33).

The full optimization problem (32) and the surrogate problem (33) were solved using MATLAB's built-in `fminsearch` together with a transformation that allows constrained optimization. The starting point was  $\mathbf{p}^0 = (100, 100, 100, 100)$  and for each parameter, the range was  $[0, 5000]$ . The stopping tolerance for optimization was set to  $\nu = 5 \cdot 10^{-4}$ . In solving the surrogate optimization problem, we employed both Algorithms 3 and 4. Our implementation will take advantage of the fact that the first subsystem  $\mathcal{H}_1(s)$  is independent of not only the parameter  $\mathbf{p}$  but also the damping positions. Therefore, for the 32 damping configurations considered, reducing  $\mathcal{H}_1(s)$  in Algorithm 3 (or sampling of  $\mathcal{H}_1(s)$  in Algorithm 4) needs to be done only once.

In Algorithm 3 for each damping configuration, we used

$$\begin{aligned} \text{termination tolerance for error bound: } & \tau = 10^{-2}; \\ \text{initial reduction dimensions: } & (r_1, r_2, r_3, r_4) = (280, 300, 480, 430). \end{aligned}$$

The reduced orders  $r_i$  were chosen based on the Hankel singular values of each subsystem. Reduced subsystem updates were performed such that each time an update was needed,  $r_i$  was increased by 15%. Similarly, in Algorithm 4 for each damping configuration, we used:

$$\begin{aligned} \text{termination tolerance for error bound } & \tau = 10^{-4}; \\ \text{initial reduced-order was set to } & 130; \\ \text{number of predetermined sampling points } \xi_1, \dots, \xi_N & \text{ was set to } N = 500. \end{aligned}$$

The sampling points  $\xi_1, \dots, \xi_N$  were chosen to be logarithmically spaced between the smallest and largest (by magnitude) undamped eigenfrequencies. We initialized VF using dominant poles [15]. During the optimization process each time that  $e(\mathcal{H}(\cdot; \mathbf{p}), \hat{\mathcal{H}}(\cdot; \mathbf{p})) > \tau$ , the order was increased by 10%.

Across all damping configurations, Algorithms 3 entered the inner while loop only in 15% of the cases and Algorithm 4 in 34% of the cases. For Algorithm 3, this means that model reduction was performed only once for most configurations. For Algorithm 4, note that it employs Algorithm 2, which resamples  $\mathcal{H}(s, \mathbf{p})$  almost at no cost, and then applies VF. Repeated application of VF constitutes only a modest cost increment since the required frequency sampling is obtained already at an earlier step. Remarkably, we have also observed that in nearly all cases that we consider, VF converges quickly. In particular, across all 32 damping configurations, application of VF for

the initial surrogate optimization step took on average 13 iterations to converge. But in the vast majority of subsequent VF application, convergence occurred often after a single iteration (93.5% of total VF applications) or two iterations (3.3% of total VF applications).

Figure 4 depicts the relative errors in the optimal gains for different damping configurations calculated by Algorithm 3 (denoted by blue squares) and Algorithm 4 (denoted by black triangles). The relative errors in the optimal gain is calculated by  $\|\mathbf{p}^* - \hat{\mathbf{p}}^*\|/\|\mathbf{p}^*\|$ , where  $\mathbf{p}^*$  and  $\hat{\mathbf{p}}^*$  denote the optimal gains calculated with, respectively, the full model (i.e., solving (32)) and the reduced model (i.e., solving (33)). The figure shows in most cases Algorithm 4 gave more accurate results.

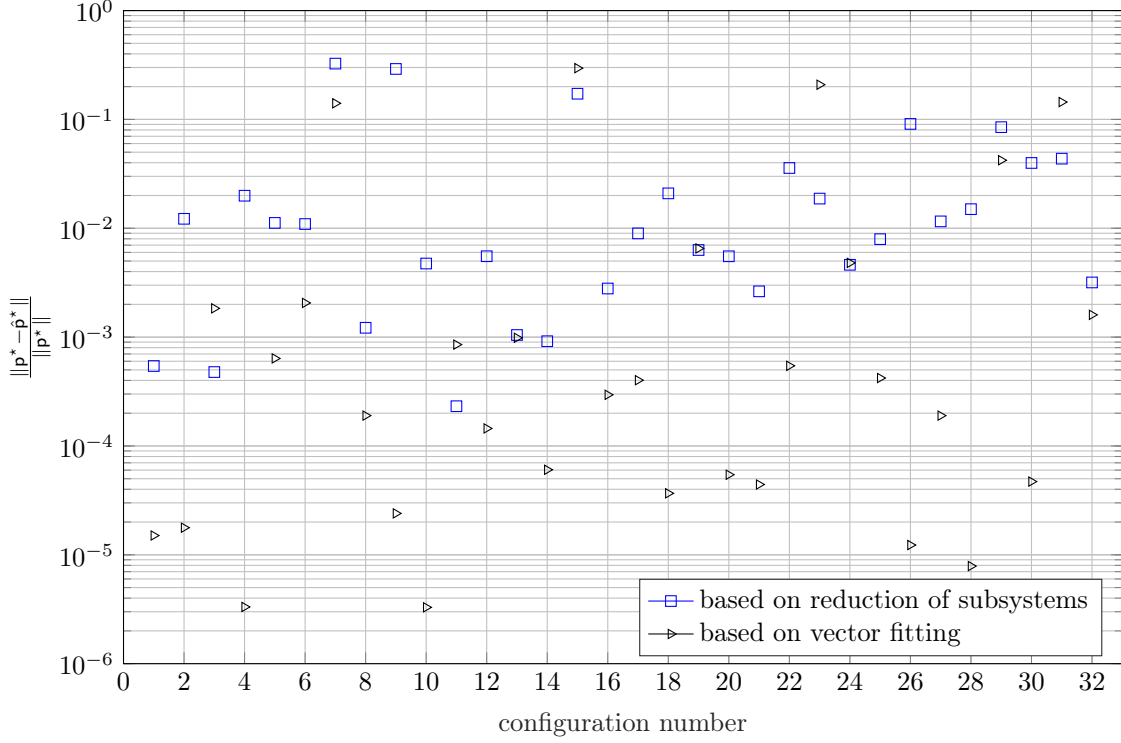


Figure 4: Relative errors in the optimal gains for Algorithm 3 and Algorithm 4

However, since the cost function, the  $\mathcal{H}_2$  norm, can be flat with respect to some damping parameters, the quality of the surrogate optimization is better illustrated in Figure 4.3 where we show the relative errors in the the cost function. For the optimal gain  $\mathbf{p}^*$  obtained by solving the full problem (32) and the optimal gain  $\hat{\mathbf{p}}^*$  obtained by solving the surrogate problem (33), the relative error is computed by  $\frac{\|\mathcal{H}(\cdot; \mathbf{p}^*)\|_{\mathcal{H}_2} - \|\mathcal{H}(\cdot; \hat{\mathbf{p}}^*)\|_{\mathcal{H}_2}}{\|\mathcal{H}(\cdot; \mathbf{p}^*)\|_{\mathcal{H}_2}}$ . These results are illustrated in In Figure 4.3. Even though both algorithms yield accurate results, the surrogate optimization with Algorithm 4 is consistently better with the largest relative error in the order of  $10^{-4}$ .

Another important quantity to measure is the speed-up compared to the full problem. Table 1 shows the average speed-ups for the optimization process obtained by both algorithms.

	Algorithm 3	Algorithm 4
Acceleration factor	7.8	60

Table 1: Acceleration factors using surrogate optimization

Both methods have optimized parameters with satisfactory relative errors with considerable acceleration of optimization process. For this damping optimization problem Algorithm 4 not only produced more accurate results but also yielded bigger speed-up than Algorithm 3. Therefore, for this problem, Algorithm 4 was more efficient. However, we also note that Algorithm 3 based on subsystem reduction include estimation of the true error  $f(\mathbf{p})$  as opposed to the sampling-based error  $e(\mathbf{p})$ , which might improve the robustness of the optimization process.

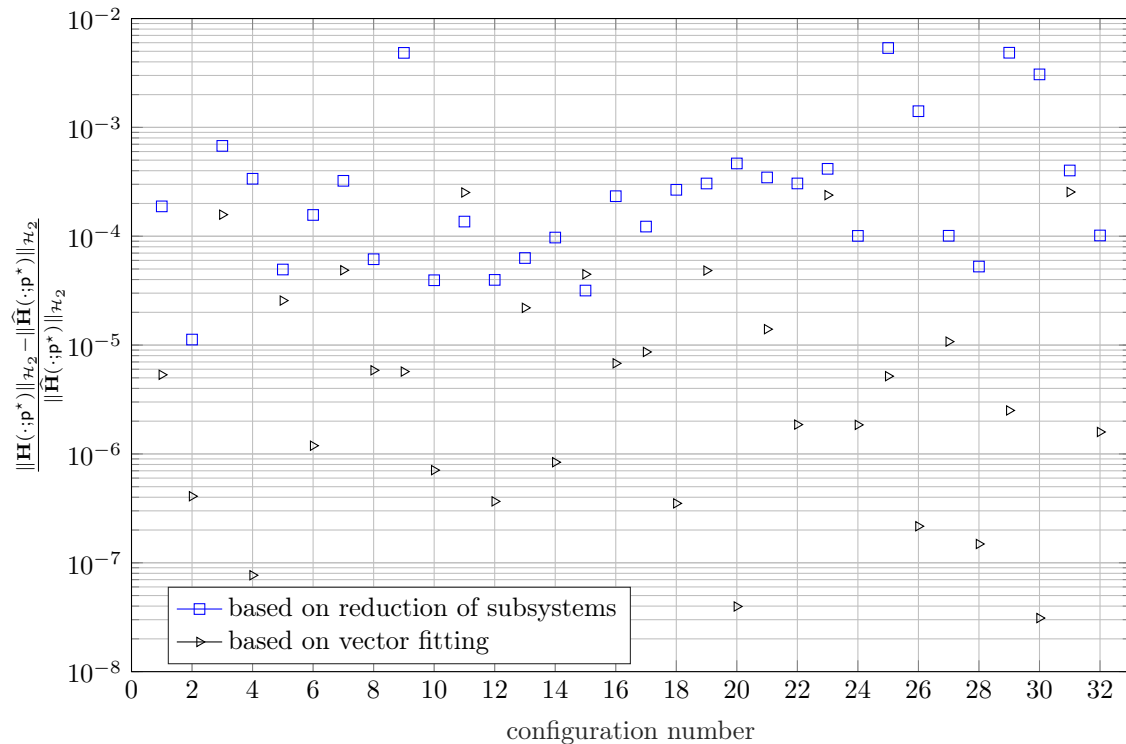


Figure 5: Relative errors for  $\mathcal{H}_2$  norm at optimal gain for Algorithm 3 and Algorithm 4

## 5 Conclusions

We have introduced a framework for producing reduced order models of dynamical systems having an affine, low-rank parametric structure. The new framework does not require any sampling in the parameter domain and instead parametrically combines intermediate subsystems that are nonparametric. Our approach can guarantee uniform stability of the aggregated reduced model across the entire parameter domain in many cases. Beyond the computational examples we provide for illustration, we show in some detail how this approach can be deployed efficiently in parameter optimization problems as well.

## Acknowledgment

This work has been supported in parts by Croatian Science Foundation under the project ‘Vibration Reduction in Mechanical Systems’ (IP-2019-04-6774) and project ‘Control of Dynamical Systems’ (IP-2016-06-2468). The work of Beattie was supported in parts by NSF through Grant DMS-1819110. The work of Gugercin was supported in parts by NSF through Grants DMS-1720257 and DMS-1923221.

## References

- [1] Alla, A., Hinze, M., Kolvenbach, P., Lass, O., Ulbrich, S.: A certified model reduction approach for robust parameter optimization with pde constraints. *Advances in Computational Mathematics* pp. 1–30 (2019)
- [2] Antil, H., Heinkenschloss, M., Hoppe, R.H.W.: Domain decomposition and balanced truncation model reduction for shape optimization of the Stokes system. *Optimization Methods and Software* **26**(4–5), 643–669 (2011)
- [3] Antoulas, A., , Beattie, C., Gugercin, S.: *Interpolatory Methods for Model Reduction*. SIAM Publications, Philadelphia, PA (2020)
- [4] Antoulas, A.: *Approximation of Large-Scale Dynamical Systems*. SIAM Publications, Philadelphia, PA (2005)



- [5] Antoulas, A., Anderson, B.: On the scalar rational interpolation problem. *IMA J. of Mathematical Control and Information* **3**, 61–88 (1986)
- [6] Antoulas, A.C., Sorensen, D.C., Gugercin, S.: A survey of model reduction methods for large-scale systems. *Contemporary Mathematics* **280**, 193–219 (2001)
- [7] Arian, E., Fahl, M., Sachs, E.: Trust-region proper orthogonal decomposition models by optimization methods. In: *Proceedings of the 41st IEEE Conference on Decision and Control*, pp. 3300–3305. Las Vegas, NV (2002)
- [8] Baur, U., Beattie, C., Benner, P.: Mapping parameters across system boundaries: parameterized model reduction with low rank variability in dynamics. *PAMM* **14**(1), 19–22 (2014)
- [9] Baur, U., Beattie, C.A., Benner, P., Gugercin, S.: Interpolatory projection methods for parameterized model reduction. *SIAM J. Sci. Comput.* **33**(5), 2489–2518 (2011)
- [10] Baur, U., Benner, P.: Model reduction for parametric systems using balanced truncation and interpolation. *at-Automatisierungstechnik* **57**(8), 411–420 (2009)
- [11] Beattie, C., Gugercin, S.: Interpolatory projection methods for structure-preserving model reduction. *Systems and Control Letters* **58**, 225–232 (2009)
- [12] Beattie, C., Gugercin, S.: A trust region method for optimal  $\mathcal{H}_2$  model reduction. In: *Proceedings of 48th IEEE Conference on Decision and Control*, pp. 5370–5375 (2009)
- [13] Benner, P., Cohen, A., Ohlberger, M., Willcox, K.: *Model Reduction and Approximation: Theory and Algorithms*. Computational Science and Engineering, SIAM Publications, Philadelphia, PA (2017)
- [14] Benner, P., Gugercin, S., Willcox, K.: A survey of projection-based model reduction methods for parametric dynamical systems. *SIAM Review* **57**(4), 483–531 (2015)
- [15] Benner, P., Kürschner, P., Tomljanović, Z., Truhar, N.: Semi-active damping optimization of vibrational systems using the parametric dominant pole algorithm. *Journal of Applied Mathematics and Mechanics* pp. 1–16 (2015). DOI:10.1002/zamm201400158.
- [16] Benner, P., Mehrmann, V., Sorensen, D.: *Dimension Reduction of Large-Scale Systems*. Lecture Notes in Computational Science and Engineering, Springer-Verlag, Berlin/Heidelberg, Germany (2005)
- [17] Benner, P., Sachs, E., Volkwein, S.: Model order reduction for PDE constrained optimization. In: G. Leugering, P. Benner, S. Engell, A. Griewank, H. Harbrecht, M. Hinze, R. Rannacher, S. Ulbrich (eds.) *Trends in PDE Constrained Optimization, International Series of Numerical Mathematics*, vol. 165, pp. 303–326. Springer International Publishing (2014). DOI 10.1007/978-3-319-05083-6\_19. URL [http://dx.doi.org/10.1007/978-3-319-05083-6\\_19](http://dx.doi.org/10.1007/978-3-319-05083-6_19)
- [18] Benner, P., Tomljanović, Z., Truhar, N.: Dimension reduction for damping optimization in linear vibrating systems. *Z. Angew. Math. Mech.* **91**(3), 179 – 191 (2011). DOI: 10.1002/zamm.201000077
- [19] Benner, P., Tomljanović, Z., Truhar, N.: Optimal Damping of Selected Eigenfrequencies Using Dimension Reduction. *Numer. Linear Algebr.* **20**(1), 1–17 (2013). DOI: 10.1002/nla.833
- [20] Berljafa, M., Güttel, S.: The RKFIT algorithm for nonlinear rational approximation. *SIAM Journal on Scientific Computing* **39**(5), 2049–2071 (2017)
- [21] Blanchini, F., Casagrande, D., Gardonio, P., Miani, S.: Constant and switching gains in semi-active damping of vibrating structures. *Int. J. Control* **85**(12), 1886–1897 (2012)
- [22] Bui-Thanh, T., Willcox, K., Ghattas, O.: Model reduction for large-scale systems with high-dimensional parametric input space. *SIAM Journal on Scientific Computing* **30**(6), 3270–3288 (2008)
- [23] Chinea, A., Grivet-Talocia, S.: On the parallelization of Vector Fitting algorithms. *IEEE Transactions on Components, Packaging and Manufacturing Technology* **1**(11), 1761–1773 (2011)

- [24] Desai, U., Pal, D.: A transformation approach to stochastic model reduction. *IEEE Transactions on Automatic Control* **29**(12), 1097–1100 (1984)
- [25] Drmač, Z., Gugercin, S., Beattie, C.: Quadrature-based vector fitting for discretized  $\mathcal{H}_2$  approximation. *SIAM J. Sci. Comp.* **37**(2), A625–A652 (2015)
- [26] Drmač, Z., Gugercin, S., Beattie, C.: Vector fitting for matrix-valued rational approximation. *SIAM Journal on Scientific Computing* **37**(5), A2346–A2379 (2015)
- [27] Egger, H., Kugler, T., Liljegren-Sailer, B., Marheineke, N., Mehrmann, V.: On structure-preserving model reduction for damped wave propagation in transport networks. *SIAM J. Sci. Comput.* **40**(1), A331–A365 (2018)
- [28] Feng, L.: Parameter independent model order reduction. *Math. Comput. Simulation* **68**, 221–234 (2005)
- [29] Feng, L., Rudnyi, E.B., Korvink, J.G.: Parametric model reduction to generate boundary condition independent compact thermal model. Technical report, IMTEK-Institute for Microsystem Technology (2004). URL <http://modelreduction.com/doc/papers/feng04THERMINIC.pdf>
- [30] Glover, K.: All optimal Hankel-norm approximations of linear multivariable systems and their  $l_\infty$ -error bounds. *International journal of control* **39**(6), 1115–1193 (1984)
- [31] Golub, G.H., Loan, C.V.F.: *Matrix Computations*. The Johns Hopkins University Press, Baltimore (1998)
- [32] Gonnet, P., Pachón, R., Trefethen, L.N.: Robust rational interpolation and least-squares. *Electronic Transactions on Numerical Analysis* **38**, 146–167 (2011)
- [33] Grimm, A.R.: Parametric dynamical systems: Transient analysis and data driven modeling. Ph.D. thesis, Virginia Tech (2018)
- [34] Grivet-Talocia, S., Gustavsen, B.: *Passive macromodeling: Theory and applications*, vol. 239. John Wiley & Sons (2015)
- [35] Gugercin, S.: An iterative SVD-Krylov based method for model reduction of large-scale dynamical systems. *Linear Algebra and Its Applications* **428**(8-9), 1964–1986 (2008)
- [36] Gugercin, S., Antoulas, A., Beattie, C.:  $\mathcal{H}_2$  model reduction for large-scale linear dynamical systems. *SIAM Journal on Matrix Analysis and Applications* **30**(2), 609–638 (2008)
- [37] Gugercin, S., Polyuga, R., Beattie, C., Schaft, A.v.: Structure-preserving tangential interpolation for model reduction of port-Hamiltonian systems. *Automatica* **48**, 1963–1974 (2012)
- [38] Gustavsen, B.: Improving the pole relocating properties of vector fitting. *IEEE Transactions on Power Delivery* **21**(3), 1587–1592 (2006)
- [39] Gustavsen, B., Semlyen, A.: Rational approximation of frequency domain responses by vector fitting. *IEEE Transactions on power delivery* **14**(3), 1052–1061 (1999)
- [40] Heinkenschloss, M., Jando, D.: Reduced order modeling for time-dependent optimization problems with initial value controls. *SIAM Journal on Scientific Computing* **40**(1), A22–A51 (2018)
- [41] Hokanson, J.M.: Projected nonlinear least squares for exponential fitting. *SIAM Journal on Scientific Computing* **39**(6), A3107–A3128 (2017)
- [42] Hund, M., Mlinarić, P., Saak, J.: An  $\mathcal{H}_2 \otimes \mathcal{L}_2$ -optimal model order reduction approach for parametric linear time-invariant systems. *Proc. Appl. Math. Mech.* **18**(1), e201800084 (2018). DOI 10.1002/pamm.201800084
- [43] Ionita, A.C., Antoulas, A.C.: Data-driven parametrized model reduction in the Loewner framework. *SIAM J. Sci. Comput.* **36**(3), 984–1007 (2014). DOI: [doi.org/10.1137/130914619](https://doi.org/10.1137/130914619)

- [44] Kunisch, K., Volkwein, S.: Proper orthogonal decomposition for optimality systems. *ESAIM: Mathematical Modelling and Numerical Analysis* **42**(1), 1–23 (2008)
- [45] Kuzmanović, I., Tomljanović, Z., Truhar, N.: Optimization of material with modal damping. *Appl Math Comput* **218**, 7326–7338 (2012)
- [46] Mayo, A., Antoulas, A.: A framework for the solution of the generalized realization problem. *Linear Algebra and Its Applications* **425**(2-3), 634–662 (2007)
- [47] Moore, B.: Principal component analysis in linear systems: Controllability, observability, and model reduction. *IEEE Transactions on Automatic Control* **26**(1), 17–32 (1981)
- [48] Müller, P., Schiehlen, W.: *Linear Vibrations*. Martinus Nijhoff Publishers (1985)
- [49] Mullis, C., Roberts, R.: Synthesis of minimum roundoff noise fixed point digital filters. *IEEE Transactions on Circuits and Systems* **23**(9), 551–562 (1976)
- [50] Nakatsukasa, Y., Sète, O., Trefethen, L.N.: The AAA algorithm for rational approximation. *SIAM Journal on Scientific Computing* **40**(3), A1494–A1522 (2018)
- [51] Nakić, I., Tomljanović, Z., Truhar, N.: Mixed control of vibrational systems. *Journal of Applied Mathematics and Mechanics* **99**(9), 1–15 (2019)
- [52] Ober, R.: Balanced parametrization of classes of linear systems. *SIAM Journal on Control and Optimization* **29**(6), 1251–1287 (1991)
- [53] Oberwolfach Benchmark Collection: Thermal model. hosted at MORwiki – Model Order Reduction Wiki (20XX). URL [http://modelreduction.org/index.php/Thermal\\_Model](http://modelreduction.org/index.php/Thermal_Model)
- [54] Opdenacker, P., Jonckheere, E.: A contraction mapping preserving balanced reduction scheme and its infinity norm error bounds. *IEEE Transactions on Circuits and Systems* **35**(2), 184–189 (1988)
- [55] van Ophem, S., Deckers, E., Desmet, W.: Parametric model order reduction without a priori sampling for low rank changes in vibro-acoustic systems. *Mechanical Systems and Signal Processing* **130**, 597–609 (2019)
- [56] Penzl, T.: Numerische simulation auf massiv parallelen rechnern. Ph.D. thesis, TU Chemnitz (1999). Algorithms for Model Reduction of Large Dynamical Systems, Tech. Rep. SFB393/99-40
- [57] Polyuga, R., van der Schaft, A.: Structure preserving moment matching for port-hamiltonian systems: Arnoldi and Lanczos. *IEEE Transactions on Automatic Control* **56**(6), 1458–1462 (2011)
- [58] Quarteroni, A., Manzoni, A., Negri, F.: *Reduced Basis Methods for Partial Differential Equations: An Introduction*. R. UNITEXT. Springer Cham (2016)
- [59] Rommes, J., Martins, N.: Computing Transfer Function Dominant Poles of Large-Scale Second-Order Dynamical Systems. *SIAM J. Sci. Comput.* **30**(4), 2137–2157 (2008)
- [60] Sanathanan, C., Koerner, J.: Transfer function synthesis as a ratio of two complex polynomials. *IEEE Trans. Autom. Control* **8**(1), 56–58 (1963)
- [61] Tomljanović, Z., Beattie, C., Gugercin, S.: Damping optimization of parameter dependent mechanical systems by rational interpolation. *Advances in Computational Mathematics* pp. 1–24 (2018)
- [62] Veselić, K.: *Damped Oscillations of Linear Systems*. Springer Lecture Notes in Mathematics, Springer-Verlag, Berlin (2011)
- [63] Yue, Y., Meerbergen, K.: Accelerating optimization of parametric linear systems by model order reduction. *SIAM Journal on Optimization* **23**(2), 1344–1370 (2012)
- [64] Yue, Y., Meerbergen, K.: Accelerating optimization of parametric linear systems by model order reduction. *SIAM Journal on Optimization* **23**(2), 1344–1370 (2013)